INVERSE ACOUSTIC SCATTERING SERIES USING THE VOLTERRA RENORMALIZATION OF THE LIPPMANN-SCHWINGER EQUATION IN ONE DIMENSION

A Thesis

Presented to

the Faculty of the Department of Mechanical Engineering

University of Houston

In Partial Fulfillment

of the Requirements for the Degree

Master of Science

in Mechanical Engineering

by

Jie Yao

August 2013

INVERSE ACOUSTIC SCATTERING SERIES USING THE VOLTERRA RENORMALIZATION OF THE LIPPMANN-SCHWINGER EQUATION IN ONE DIMENSION

Jie Yao

Approved:

Chair of the Committee
Donald Kouri, Professor
Dept. of Physics

Committee Members:

Fazle Hussain, Professor
Dept. of Mechanical Engineering

Bernhard Bodmann,
Associate Professor
Dept. of Mathematics

Suresh K. Khator, Associate Dean
Cullen College of Engineering

Pradeep Sharma, Chair
Dept. of Mechanical Engineering

Acknowledgements

I feel very lucky to have met and worked with many people and professors who have given me lots of help during the past year at UH. Among all of them, my two advisors, Professor Fazle Hussain and Professor Donald Kouri affected me the most. First, I wish to express my deepest gratitude to Dr. Hussain for recommending me to Dr. Kouri. I am sincerely grateful to Dr. Kouri, not only for his support on my research, but for his advice, and guidance through my studies.

A special debt of gratitude goes to Anne-Cécile for helping me with the project. She gave me a lot of instructions and help during the past few months. It was an enjoyable time to work with her.

I am much indebted to my parents for everything I may have achieved. Even though they could not give me any instruction on research, they give me the impetus to keep moving forward. I wish to express my profound gratitude to Qiushuo Su. She is the one who gave me the chance to come here to pursue my study. She deserves all the glories that I have achieved. I want to express my genuine appreciation to her for her help, support and continuous encouragement during the past five years.

INVERSE ACOUSTIC SCATTERING SERIES USING THE VOLTERRA RENORMALIZATION OF THE LIPPMANN-SCHWINGER EQUATION IN ONE DIMENSION

An Abstract

of a

Thesis

Presented to

the Faculty of the Department of Mechanical Engineering

University of Houston

In Partial Fulfillment

of the Requirements for the Degree

Master of Science

in Mechanical Engineering

by

Jie Yao

August 2013

Abstract

The inverse scattering problem has enormous importance both for practical and theoretical applications, such as seismic exploration, nondestructive testing, and medical imaging. Based on the early work of Jost and Kohn [1], Moses [2], Razavy [3] and Prosser [4], Weglein and co-workers have pioneered inverse scattering series methods that require no assumed propagation velocity model. Kouri and Vijay formulated the 1-D acoustic scattering series in terms of a Volterra kernel with reflection and transmission data [5]. It can be further proved that the Born-Neumann series solution of the Volterra equation converges absolutely, irrespective of the strength of the velocity interaction. Following this previous work of Kouri, higher orders of the Volterra Inverse Scattering Series (VISS) with reflection and transmission data (R_k / T_k) are analyzed here. In addition, for the seismic exploration applications, we also extended the VISS approach to the case where only the reflection data is available. The cases of single square barriers or wells and Gauss barriers and wells are studied to illustrate how well the Volterra Inverse Scattering Series performs the inversion. The results demonstrate that the Volterra inverse scattering series method is an effective tool in inverse scattering.

Table of Contents

List of Figures

List of Tables

CHAPTER 1 INTRODUCTION AND BACKGROUND

1.1 INTRODUCTION, MOTIVATION AND BACKGROUND

Scattering theory is an important tool in studying the structure and dynamics of matter. The fields of application are numerous, and as diverse as quantum physics, classical physics, mechanical engineering, electrical engineering and medical imaging. In all these fields, scattering theory is used in one form or another to obtain information about the system under investigation. The forward scattering problem involves determining the scattered field when the system interaction is known. The inverse scattering problem, on the other hand, is the reverse: from the measured scattered field, satisfying certain boundary conditions, one must determine the scattering interaction. Whereas forward scattering is quite well understood, the inverse scattering problem still attracts attention in all the major branches of science and engineering. The task underlying every inverse scattering problem, regardless of the field of application, is the development of a procedure that determines the properties of the scatterers from the scattering data.

1.1.1 Introduction to Seismic exploration

In the seismic exploration, a controlled man-made source of acoustic energy on or near the surface sends an incident pulse into the subsurface. When the wave reaches reflectors, (i.e., rapid changes in earth properties), a portion of the wave will be reflected to the surface where it will be recorded by numerous receivers. The reflected wave contains information about the source that created it, the medium that the wave traveled through and the reflectors that caused part of the wave to return. The objective of seismic exploration is to reveal subsurface earth properties from the recorded seismic data.

The current need for more effective and reliable techniques for seismic data processing algorithms is driven by the factor that the quality of the image obtained from the processed seismic data has a direct influence on our ability and the cost of finding hydrocarbon

targets.

The problem of determining earth material properties from seismic reflection data is an inverse scattering problem and, specifically, a nonlinear one. Current methods can in general be classified into two categories [6]: the first methods used in exploration seismology could be viewed as different realizations of a linear approximation to inverse scattering; namely the inverse Born approximation [7, 8, 9]. The second methods are non-linear inverse scattering series approaches which were first introduced and adapted to exploration seismology in the early 1980s. Practical algorithms were first demonstrated by Weglein in 1997 [10].

1.1.2 Introduction to inverse scattering series

The inverse scattering series methods were first developed in 1952 by Jost and Kohn[1], Moses [2], Prosser [4] and Razavy [3] and were introduced by Weglein [10] to migrate seismic data to the correct depth in seismic exploration. Comparing with some common imaging methods, inverse scattering series methods have the advantage of making it possible to image the sublayers of the earth with a reference background velocity that is valid near the earth's surface. These methods do not need more knowledge of the sublayer. As mentioned in Weglein [11], the inversion process can be thought of as performing four tasks: (1) free surface multiple removal, (2) internal multiple removal, (3) location of reflectors in space, and (4) identification of medium property changes across reflectors. Following this idea, Weglein and co-workers extract task-specific subseries from the inverse scattering series and prove them to be responsible for locating reflectors at the correct spatial location. They isolated a leading order inverse-scattering series [12] and extended the algorithms to three dimensions [13]. Inverse scattering series methods have a significant advantage in comparison to other data inversion methods like Full Waveform Inversion [14, 15]. The inverse scattering series is the only inversion method that does not need to assume the actual and estimated reference media to be equal. The method is non-iterative in the sense that the

reference medium is never updated.

The question in considering a series solution is the issue of convergence followed closely by the question of the rate of convergence. The inverse scattering series method is limited by the finite radius of convergence of the Born-Neumann series of the acoustic Lippmann-Schwinger equation. Indeed, because in seismic physics, the interaction increases as the square of the frequency; there is always a region where the series never converges. If the strength of the spatial part of the interaction is large, non-convergence occurs at even lower frequencies. Kouri and co-workers [5] proposed to apply the renormalization transformation of the Lippmann-Schwinger equation into a Volterra equation [16] to overcome the convergence limitation of the inverse acoustic scattering series. The Volterra inverse scattering series converges absolutely and uniformly on any compact set independent of the strength of the scattering interaction and the frequency.

1.2 OVERVIEW OF THE THESIS

My Master's thesis is part of a long-term research project aimed at solving the problem of inverse scattering for acoustic wave propagation in the earth's subsurface. We are in the beginning stage, and therefore we are investigating the use of Volterra Inverse Scattering Series (VISS) for one dimensional acoustic scattering problems. Even though the Earth is a 3-D elastic medium, it is still significant to study the simple 1-D acoustic problem. The reason for this is that an algorithm is worth the additional labor and mathematical formalism involved in its generalization to more complex wave propagation, only if it shows significant effectiveness for 1-D acoustic models. I follow closely the analysis of Kouri and Vijay [5] where they presented the Volterra inverse scattering series using both reflection and transmission data (R_k / T_k). In this thesis, I use this approach to further understand how the Volterra inverse scattering series converges. In addition, for seismic exploration, I also extend the Volterra inverse scattering series method to the sole use of reflection data (R_k). Similar to other studies, we employ the Volterra inverse scattering se-

ries method to consider the simplest situation. This is a 1-D normal incidence experiment in a layered acoustic medium, in which the velocity is constant in each layer. Secondly, we also test our method for velocity interaction that varies as a Gaussian with depth.

CHAPTER 2 THE INVERSE SCATTERING USING RENORMALIZATION OF ONE DIMENSION ACOUSTIC LIPPMANN-SCHWINGER EQUATION

The inverse scattering problem consists of reconstructing the interaction V from the scattering data (the ratio of R_k/T_k) or from R_k alone. In this section, we develop a Volterra inverse scattering series to build the velocity interaction V from the measured data. This chapter is organized as follows: first we give a brief review of the mathematical framework of acoustic scattering; next we obtain the Volterra Inverse Scattering Series for R_k/T_k data by renormalizing the Lippmann-Schwinger equation for acoustic wave in one dimension [5]. Then, for seismic exploration, we extend the Volterra Inverse Scattering Series method to solely using R_k data.

2.1 ACOUSTIC SCATTERING MODEL

Consider a 1D acoustic medium, where the velocity is a function of depth, $c = c(z)$, that is connected to a homogeneous reference medium with wave velocity c_0. The 1D wave equation for scattering of the pressure wave P, with angular frequency ω and corresponding wave number $k = \omega/c_0$, in a velocity interaction $V(z) = 1 - \frac{c_0^2(z)}{c^2(z)}$ (which characterizes the difference between the reference and actual medium) is:

$$(\frac{\partial}{\partial z^2} + k^2)P \;\; = \;\; k^2 V P. \tag{2.1}$$

The forward problem associated with Eq.(2.1) is stated as follows: given the interaction $V(z)$, find the solution P that satisfies the prescribed boundary conditions. As usual in scattering theory, the interaction V is assumed to be compactly supported or tend to zero as $|z|$ becomes large, which means that V is assumed to vanish asymptotically at infinity ($V \to 0$, as $z \to \pm\infty$). In the asymptotic regions, the wave pressure P is merely proportional to a free plane wave described by $e^{\pm ikz}$. An integral representation for the pressure wave can be found if we write Eq.(2.1) as an integral equation. To this end, we

can construct the Green's function for the Helmholtz equation:

$$(\frac{\partial}{\partial z^2} + k^2)G_0(z,z') = \delta(z-z'). \tag{2.2}$$

The solution of this equation with an "outgoing wave" boundary condition yields the one dimensional causal free Green's function [3]:

$$G_0^+ = -\frac{i}{2k}e^{ik|z-z'|}. \tag{2.3}$$

Then the Lippmann-Schwinger integral equation for the pressure wave can be represented as:

$$P_k^+(z) = e^{ikz} + \int_{-\infty}^{\infty} dz' G_{0k}^+(z,z')V(z')P_k^+(z'), \tag{2.4}$$

where G_{0k}^+ is the causal free Green's function multiplied by a factor of k^2:

$$G_{0k}^+ = -\frac{ik}{2}e^{ik|z-z'|}. \tag{2.5}$$

In 1D scattering, the reflection scattering amplitude is given by [17]:

$$R_k = -\frac{ik}{2}\int_{-\infty}^{\infty} dz' e^{ikz'}V(z')P_k^+(z'). \tag{2.6}$$

The transmission amplitude T_k is given by:

$$T_k = 1 - \frac{ik}{2}\int_{-\infty}^{\infty} dz' e^{-ikz'}V(z')P_k^+(z'). \tag{2.7}$$

2.2 THE VOLTERRA INVERSE SCATTERING SERIES FOR R_k/T_k DATA

2.2.1 Renormalization of the Lippmann-Schwinger equation for 1-D acoustic scattering with R_k/T_k data

The renormalization transformation of the Lippmann-Schwinger equation (Eq.2.4) to a Volterra equation results from eliminating the $|z-z'|$ argument in the causal Green's

function in Eq.(2.5). This is done by dividing the integration over z' into segments from $-\infty$ to z and from z to ∞:

$$P_k^+(z) = e^{ikz} - \frac{ik}{2}\int_{-\infty}^{z} dz' e^{ik(z-z')}V(z')P_k^+(z') - \frac{ik}{2}\int_{z}^{\infty} dz' e^{ik(z'-z)}V(z')P_k^+(z'). \tag{2.8}$$

One then adds and substracts $-(ik/2)\int_z^\infty dz' e^{ik(z-z')}V(z')P_k^+(z')$, and after simple manipulation, one can obtains

$$\begin{aligned} P_k^+(z) &= e^{ikz} - \frac{ik}{2}\int_{-\infty}^{\infty} dz' e^{ik(z-z')}V(z')P_k^+(z') \\ &\quad - \frac{ik}{2}\int_{z}^{\infty} dz'[e^{ik(z'-z)} - e^{-ik(z'-z)}]V(z')P_k^+(z'). \end{aligned} \tag{2.9}$$

It is easily verified that this is equivalent to writing $G_{0k}^+(z,z')$ as

$$G_{0k}^+(z,z') = \widetilde{G}_{0k}(z,z') - \frac{ik}{2}e^{ik(z-z')}, \tag{2.10}$$

where

$$\begin{aligned} \widetilde{G}_{0k}(z,z') &= -\frac{ik}{2}[e^{ik(z'-z)} - e^{-ik(z'-z)}] \\ &= \begin{cases} k\sin[k(z-z')], & z' > z \\ 0, & z' \le z \end{cases}. \end{aligned} \tag{2.11}$$

Thus

$$\widetilde{G}_{0k}(z,z') = k\sin[k(z'-z)]\eta(z'-z), \tag{2.12}$$

where $\eta(z)$ is the heaviside function ($\eta = 0$ for $z < 0$, $\eta = 1$ for $z \ge 0$).

Combining Eq.(2.7), (2.9) and (2.11), we obtain:

$$\begin{aligned} P_k^+(z) &= T_k e^{ikz} + \int_{-\infty}^{\infty} dz' \widetilde{G}_{0k}(z,z')V(z')P_k^+(z') \\ &= T_k e^{ikz} + k\int_{z}^{\infty} dz' \sin[k(z'-z)]V(z')P_k^+(z'), \end{aligned} \tag{2.13}$$

which can be recognized as an inhomogeneous Volterra integral equation of the second kind [18].

2.2.2 The Volterra Inverse Scattering Series for V with R_k/T_k

To solve Eq.(2.13), assume the solution has the following form:

$$P_k^+(z) = P_k(z)T_k. \tag{2.14}$$

Substituting Eq.(2.14) into Eq.(2.13), we obtain

$$\begin{aligned} P_k(z) &= e^{ikz} + \int_{-\infty}^{\infty} dz' \widetilde{G}_{0k}(z,z')V(z')P_k(z') \\ &= e^{ikz} + k\int_{z}^{\infty} dz' \sin[k(z'-z)]V(z')P_k(z'). \end{aligned} \tag{2.15}$$

Iterating Eq.(2.15), we can get the Born-Neumann series for P_k [18]:

$$P_k(z) = \sum_{n=0}^{\infty} (\widetilde{G}_{0k}V)^n |k>, \tag{2.16}$$

where $|k>$ is a shorthand notation for e^{ikz}.

Because of the triangular nature of $\widetilde{G}_{0k}$, $P_k(z)$ converges absolutely and uniformly on any compact set of z or k, provided V is bounded and decays faster than $1/z^2$ for large $|z|$ (Refer to Appendix A). Substituting Eq.(2.16) into Eq.(2.6), we can get

$$\frac{2i}{k}\frac{R_k}{T_k} = \int_{-\infty}^{\infty} dz' e^{ikz'} V(z') \sum_{n=0}^{\infty} (\widetilde{G}_{0k}V)^n |k> . \tag{2.17}$$

To solve the above equation, we replace $\frac{2i}{k}\frac{R_k}{T_k}$ in Eq.(2.17) by $\epsilon\frac{2i}{k}\frac{R_k}{T_k}$, where ϵ is an "ordering parameter," which ultimately is set equal to one. Furthermore, we can also express V as a power series in orders of the data (The convergence of power series of V is different from the convergence of the Born-Neumann series of P_k, and has not been considered in this thesis):

$$V = \sum_{j=1}^{\infty} \epsilon^j V_j. \tag{2.18}$$

Substituting into Eq.(2.17), we can get:

$$\epsilon\frac{2i}{k}\frac{R_k}{T_k} = \int_{-\infty}^{\infty} dz' e^{ikz'} \sum_{j=1}^{\infty} \epsilon^j V_j \sum_{n=0}^{\infty} (\widetilde{G}_{0k} \sum_{j'=1}^{\infty} \epsilon^{j'} V_{j'})^n |k> . \tag{2.19}$$

Collecting coefficients of each power of ϵ yields:

$$\begin{aligned}
\varepsilon^1 &: V_1(2k) = \frac{2i}{k}\frac{R_k}{T_k}, && (2.20)\\
\varepsilon^2 &: V_2(2k) = - < -k|V_1\widetilde{G}_{0k}V_1|k >, && (2.21)\\
\varepsilon^3 &: V_3(2k) = - < -k|V_2\widetilde{G}_{0k}V_1|k > - < -k|V_1\widetilde{G}_{0k}V_2|k > \\
&\qquad - < -k|V_1\widetilde{G}_{0k}V_1\widetilde{G}_{0k}V_1|k >, && (2.22)
\end{aligned}$$

etc. The form of the Volterra inverse series with R_k/T_k is identical with Weglein's [10], except for the expression for the first order and the Green's function. Weglein's equations replace $\widetilde{G}_{0k}$ with G^+_{0k} (Eq.(2.10)). These matrix element expressions are first evaluated in the k representation and the results are subsequently transformed to the z representation. By the inverse Fourier transform of Eq.(2.20) to the space domain, we obtain $V_1(z)$. The result is

$$V_1(z) = \frac{2i}{\pi}\int_{-\infty}^{\infty} dk \frac{e^{-2ikz}R_k}{kT_k}. \qquad (2.23)$$

Similarly, we can obtain the higher order contributions, $V_j(z), j = 2,3,\cdots$. For example, we can compute $V_2(z)$ according to

$$\begin{aligned}
V_2(z) &= \frac{1}{\pi}\int_{-\infty}^{\infty} dk e^{-2ikz}V_2(2k)\\
&= \frac{1}{\pi}\int_{-\infty}^{\infty} dk e^{-2ikz}\int_{-\infty}^{\infty} dz'\int_{-\infty}^{\infty} dz'' e^{ik(z'+z'')}V_1(z')\widetilde{G}_{0k}(z,z'')V_1(z'').
\end{aligned} \qquad (2.24)$$

2.3 THE VOLTERRA INVERSE SCATTERING SERIES FOR R_k DATA

For seismic scattering, we can only measure the reflection data. Hence, it's necessary to develop an approach using solely the reflection data in order to invert seismic data.

2.3.1 Renormalization of the Lippmann-Schwinger equation for 1-D acoustic scattering with R_k data

One now adds and substracts $-(ik/2)\int_{-\infty}^{z} dz' e^{ik(z'-z)} V(z') P_k^+(z')$ to Eq.(2.8), and after simple manipulation, one can obtains

$$\begin{aligned} P_k^+(z) &= e^{ikz} - \frac{ik}{2}\int_{-\infty}^{\infty} dz' e^{ik(z'-z)} V(z') P_k^+(z') \\ &\quad - \frac{ik}{2}\int_{-\infty}^{z} dz' [e^{ik(z-z')} - e^{-ik(z-z')}] V(z') P_k^+(z'). \end{aligned} \tag{2.25}$$

Combining Eq.(2.6) and (2.25), we obtain

$$\begin{aligned} P_k^+(z) &= e^{ikz} + R_k e^{-ikz} + \int_{-\infty}^{\infty} dz' \widetilde{G}_{0k}(z,z') V(z') P_k^+(z') \\ &= e^{ikz} + R_k e^{-ikz} + k\int_{-\infty}^{z} dz' k \sin[k(z-z')] V(z') P_k^+(z'), \end{aligned} \tag{2.26}$$

where the new Green's function is given by

$$\begin{aligned} \widetilde{G}_{0k}(z,z') &= -\frac{ik}{2}[e^{ik(z-z')} - e^{-ik(z-z')}] \\ &= \begin{cases} k\sin[k(z'-z)], & z' < z \\ 0, & z' \geq z \end{cases}. \end{aligned} \tag{2.27}$$

Or

$$\widetilde{G}_{0k}(z,z') = k\sin[k(z-z')]\eta(z-z'). \tag{2.28}$$

Eq.(2.26) is also an inhomogeneous Volterra integral equation of the second kind.

2.3.2 The Volterra inverse scattering series for V with R_k data

To solve Eq.(2.26), we can try a solution of the following form:

$$P_k^+(z) = P_{1k}(z) + R_k P_{2k}(z). \tag{2.29}$$

Plugging Eq.(2.29) into Eq.(2.26), we obtain

$$\begin{aligned} P_k^+(z) &= P_{1k}(z) + R_k P_{2k}(z) \\ &= e^{ikz} + R_k e^{-ikz} + \int_{-\infty}^{\infty} dz' \widetilde{G}_{0k}(z,z') V(z') [P_{1k}(z) + R_k P_{2k}(z)]. \end{aligned} \tag{2.30}$$

This is satisfied if:

$$\begin{aligned} P_{1k}(z) &= e^{ikz} + \int_{-\infty}^{z} dz' \widetilde{G}_{0k}(z,z') V(z') P_{1k}(z') \\ &= e^{ikz} + k \int_{-\infty}^{z} dz' \sin[k(z-z')] V(z') P_{1k}(z'), \qquad (2.31) \\ P_{2k}(z) &= e^{-ikz} + \int_{-\infty}^{z} dz' \widetilde{G}_{0k}(z,z') V(z') P_{2k}(z') \\ &= e^{-ikz} + k \int_{-\infty}^{z} dz' \sin[k(z-z')] V(z') P_{2k}(z'). \qquad (2.32) \end{aligned}$$

We stress that

$$P_{2k}(z) = P_{1k}^{*}(z). \qquad (2.33)$$

The Born-Neumann series solution for $P_{1k}(z)$ can be represented as:

$$P_{1k}(z) = \sum_{n=0}^{\infty} (\widetilde{G}_{0k} V)^n |k> . \qquad (2.34)$$

Combining Eqs.(2.6),(2.31) and (2.34), we find that

$$R_k = -\frac{ik}{2} \int_{-\infty}^{\infty} dz' e^{ikz'} V(z') [\sum_{n=0}^{\infty} (\widetilde{G}_{0k} V)^n |k> + R_k \sum_{n=0}^{\infty} (\widetilde{G}_{0k} V)^n | -k >]. \qquad (2.35)$$

To solve the above equation, we replace R_k in Eq.(2.35) by ϵR_k, where now ϵ denotes first order in the data R_k. Furthermore, we can also express V as a power series in order of the data:

$$V = \sum_{j=1}^{\infty} \epsilon^j V_j. \qquad (2.36)$$

Substituting into Eq.(2.35), we obtain

$$\begin{aligned} \epsilon R_k &= -\frac{ik}{2} \int_{-\infty}^{\infty} dz' e^{ikz'} \sum_{j=1}^{\infty} \epsilon^j V_j [\sum_{n=0}^{\infty} (\widetilde{G}_{0k} \sum_{j'=1}^{\infty} \epsilon^{j'} V_{j'})^n |k> \\ &\quad + \epsilon R_k \sum_{n'=0}^{\infty} (\widetilde{G}_{0k} \sum_{j''=1}^{\infty} \epsilon^{j''} V_j'')^{n'} | -k >], \qquad (2.37) \end{aligned}$$

here, $|-k>$ is e^{-ikz}.

Collecting coefficients of each power of ϵ, we obtain

$$\varepsilon^1 \;:\; V_1(2k) = \frac{2iR_k}{k}, \tag{2.38}$$

$$\varepsilon^2 \;:\; V_2(2k) = -<-k|V_1\widetilde{G}_{0k}V_1|k> - R_k<-k|V_1|-k>, \tag{2.39}$$

$$\begin{aligned}\varepsilon^3 \;:\; V_3(2k) = &-<-k|V_2\widetilde{G}_{0k}V_1|k> - <-k|V_1\widetilde{G}_{0k}V_2|k> \\ &-<-k|V_1\widetilde{G}_{0k}V_1\widetilde{G}_{0k}V_1|k> \\ &- R_k<-k|V_2|-k> - R_k<-k|V_1\widetilde{G}_{0k}V_1|-k>,\end{aligned} \tag{2.40}$$

etc. By the inverse Fourier transform of Eq.(2.38)to the space domain, we can get $V_1(z)$. The result is

$$V_1(z) \;=\; \frac{2i}{\pi}\int_{-\infty}^{\infty} dk \frac{R_k e^{-2ikz}}{k}. \tag{2.41}$$

This expression for $V_1(z)$ is identical with the result obtained by Razavy [3] and Weglein [10], which is recognized as a direct Fourier transform of the reflection data R_k, divided by k. The forms for the high order series terms $V_j, j > 1$ differ from Weglein's [10] in two ways: the first is the Green's function. The second is the fact that we have extra terms that contain R_k.

2.4 THE CONVERGENCE FOR THE VOLTERRA INVERSE SCATTERING SERIES

Any series naturally raise the issue of convergence. A body of work by Prosser [4, 19, 20, 21] has formally addressed the topic of convergence of the inverse series including the existence and uniqueness of its solution. He shows that convergence of the inverse series based on the Fredholm integral equation requires that the scattering interaction should be sufficiently weak to allow convergence of the forward series. This is the series that results from iterating the Lippmann-Schwinger equation directly, thus involving G_{0k}^{+}. It is indeed

found that the entire series for a simple 1-D acoustic model converges slowly or does not converge at all unless reference medium properties are chosen to be very close to the actual medium properties. Based on these tests, the radius of convergence was considered to be too small for the series to be of direct practical use when no a priori information is supplied. On the other hand, we can prove that the Born-Neumann series for either of the Volterra integral equations are absolutely convergent, independent of the strength of the interaction. For the Volterra-based inverse series, the kernel can be represented as

$$\begin{aligned} \gamma K(z,z') &= k\gamma \sin[k(z'-z)]V(z'),\ z<z' && (2.42)\\ &= 0,\ z>z'. && (2.43) \end{aligned}$$

The Fredholm determinant can be expressed as an infinite series of the form:

$$D(\gamma) = \sum_{n=0}^{\infty} TrK^n(-\gamma)^n. \quad (2.44)$$

For the Volterra kernel above, we can verify that

$$TrK^n = \delta_{n0}, \quad (2.45)$$

and then it is easy to verify that the fredholm determinant for such kernel is

$$D(\gamma) = 1. \quad (2.46)$$

Furthermore, by use of Hadamard's theorem [18, 22], it is easily proved that the infinite series for the Fredholm minor converges absolutely and uniformly for γ in the entire complex plane. Details are given in Appendix A. We can conclude that iterative solution of Volterra integral equation possess the most robust convergence.

CHAPTER 3 THE APPLICATION OF VOLTERRA INVERSE SCATTERING SERIES TO THE SQUARE WELL OR BARRIER INTERACTION

In this chapter, we will apply our Volterra inverse scattering series to a finite single square well or barrier interaction (see figure 3.1). The expression for the interaction is

$$V(z) = V_0\eta(z)\eta(a-z), \tag{3.1}$$

where $\eta(z)$ is again the heaviside function.

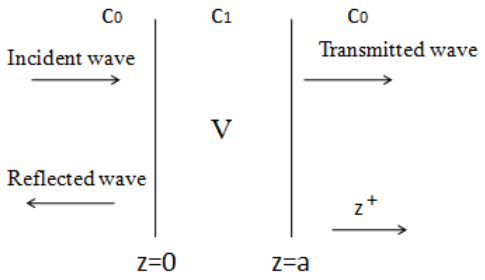

Figure 3.1. Single layer with velocity C_1

For this simple case, the reflection and transmission amplitudes can be obtained analytically.

3.1 THE ANALYTICAL REFLECTION AND TRANSMISSION COEFFICIENT OF THE SQUARE WELL OR BARRIER INTERACTION

The Helmholtz equation for the square well or barrier velocity contrast can be represented as

$$(\frac{\partial}{\partial z^2} + k^2)P = k^2VP, \tag{3.2}$$

with

$$V(z) = \begin{cases} V_0, & 0 < z < a \\ 0, & Otherwise \end{cases}. \tag{3.3}$$

Here, $V_0 = 1 - \frac{c_0^2}{c_1^2}$.Where the case $V_0 < 0$ corresponds to a square well, the case $0 < V_0 < 1$ corresponds to a barrier.

The solution for the pressure wave of the above equation can be represented in this form [23],

$$P(z) = \begin{cases} e^{ikz} + R_k e^{-ikz}, & z < 0 \\ A_1 e^{ik'z} + A_2 e^{ik'z}, & 0 < z < a \\ T_k e^{ikz}, & z > a \end{cases}. \tag{3.4}$$

At $z = 0$ and $z = a$, the pressure wave and its first derivative must be continuous[24]. Therefore the following equations must apply:

$$R_k = A_1 + A_2, \tag{3.5}$$

$$ik - ikR_k = ik'A_1 - ik'A_2, \tag{3.6}$$

$$A_1 e^{ika} + A_2 e^{-ika} = T_k e^{ika}, \tag{3.7}$$

$$ik'A_1 e^{ika} - ik'A_2 e^{-ika} = ikT_k e^{ika}. \tag{3.8}$$

From Eq.(3.5)-(3.8), we have

$$R_k = \frac{V_0 \sin(ak\sqrt{1-V_0})}{(2-V_0)\sin(ak\sqrt{1-V_0}) + 2i\sqrt{1-V_0}\cos(ak\sqrt{1-V_0})}, \tag{3.9}$$

$$T_k = \frac{2\sqrt{1-V_0}e^{-ika}}{V_0 \sin(ka\sqrt{1-V_0})} R_k. \tag{3.10}$$

3.2 RESULTS FOR VISS WITH R_k / T_k

Using the Volterra inverse scattering series with R_k / T_k(Eq.(2.20)), we obtain the results for the first three orders for the square well or barrier (The details of the computation

are given in appendix B),

$$
\begin{aligned}
V_1(z) &= \frac{V_0}{\sqrt{1-V_0}}\eta(z-z_1)\eta(z_2-z), && (3.11)\\
V_2(z) &= -\frac{V_0^2}{2(1-V_0)}\eta(z-z_1)\eta(z_2-z) \\
&+ \frac{V_0^2}{4(1-V_0)}(z_2-z_1)[\delta(z_1-z)+\delta(z_2-z)], && (3.12)\\
V_3(z) &= \frac{1}{8}(\frac{V_0}{\sqrt{1-V_0}})^3\eta(z-z_1)\eta(z_2-z) \\
&- \frac{1}{16}(\frac{V_0}{\sqrt{1-V_0}})^3(z_2-z_1)[\delta(z_1-z)+\delta(z_2-z)] \\
&+ \frac{1}{32}(\frac{V_0}{\sqrt{1-V_0}})^3(z_2-z_1)^2[\delta'(z_2-z)-\delta'(z_1-z)], && (3.13)
\end{aligned}
$$

where $\eta(z)$ is the Heaviside function and $z_1 = \frac{a}{2}(1-\sqrt{1-V_0})$, $z_2 = \frac{a}{2}(1+\sqrt{1-V_0})$.

For a barrier, $0 < V_0 < 1$ so that the first-order result has a higher barrier than the true one. For a well, $V_0 < 0$ and the first order result is shallower than the true well. Thus, although the first-order result has the correct analytical form of a square well or barrier, it has an incorrect width and height (or depth). For the high orders, the results contain two contributions: (1) The Heaviside terms (similar to the first order), (2) the Dirac-δ function and its derivatives terms. Similar to Weglein's subseries idea, each part in our series contains one specific task. For the Heaviside term, it can be used to determine the interaction magnitude. The Dirac-δ function and its derivatives terms perform the task of locating the reflectors (i.e., the beginning and ending of the barrier or well).

3.2.1 Velocity estimation

For acoustic inverse scattering, the main issues are how can we achieve accurate imaging at depth and also get a proper velocity estimation. For different values of V_0, we compare the plots of the exact barrier or well, and the Heaviside terms of the first three orders $V_j(z)$ obtained through the Volterra Inverse Scattering Series with R_k/ T_k data.

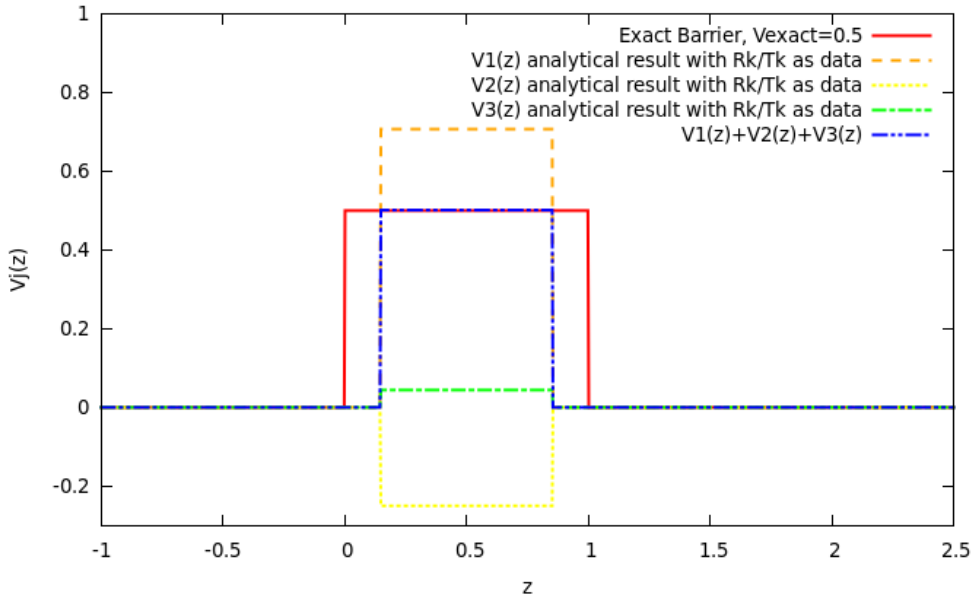

Figure 3.2. Comparison of $V_j(z)$ obtained through the Volterra inverse scattering series in R_k/T_k and the exact barrier. Square barrier test case: $V_0 = 0.5$, $a = 1.0$.

We observe that for low contrast between the true velocity and the reference velocity (cases $V_0 = 0.5$ and $V_0 = -2.0$), the series V_j shows excellent convergence after summing the first three orders. Note that for $V_0 = 0.5$, one has $c_1 = \sqrt{2}c_0$ and for $V_0 = -2$, one has $c_1 = c_0/\sqrt{3}$.

Moreover, if we denote the height of the V_j by $A(V_j)$, we have $|A(V_1)| > |A(V_2)| > |A(V_3)|$ which agrees with our assumption that V_j corresponds to the j^{th} order of the data. Figure 3.6 shows the height convergence as a function of the number of summed V_j higher order terms. Table 3.2.1 shows the amplitude error as a function of the number of V_j terms included.

Although the differences between the actual velocity interaction and the sum of the first three orders increases for higher velocity contrast(case $V_0 = -3$ and $V_0 = -4$), it is still satisfying that the percent error is actually rather small. Furthermore, we can compute more terms if we want to reach higher accuracy, since it has been proved in Chapter 2 that our Volterra inverse scattering series converges absolutely and uniformly.

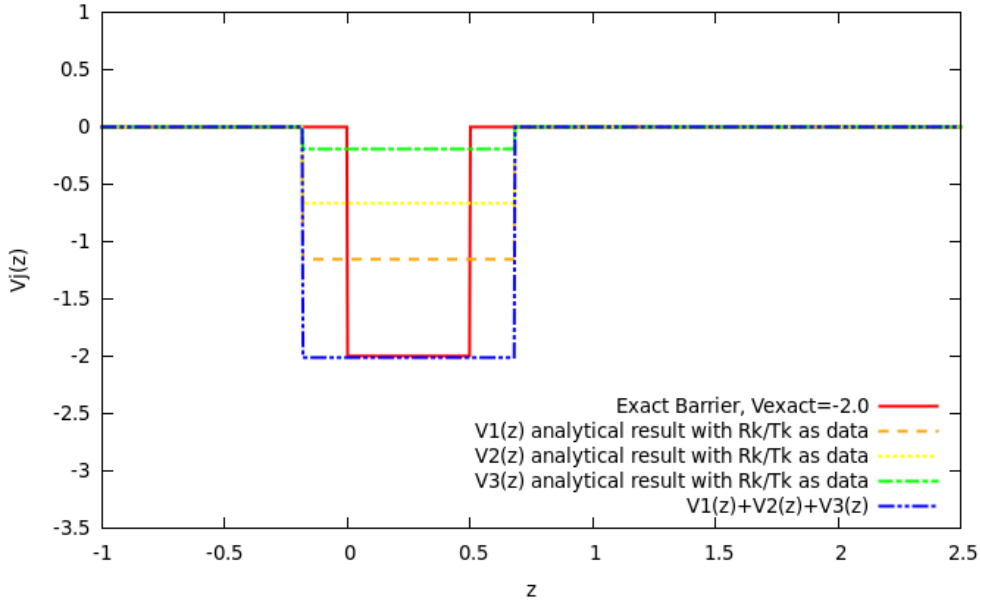

Figure 3.3. Comparison of $V_j(z)$ obtained through the Volterra inverse scattering series in R_k/T_k and the exact barrier. Square barrier test case: $V_0 = -2.0$, $a = 0.5$.

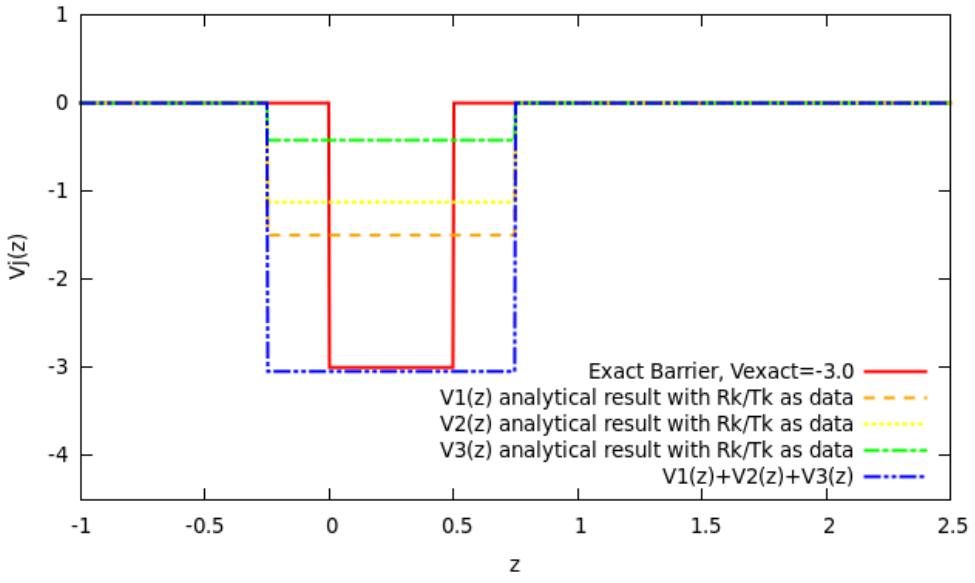

Figure 3.4. Comparison of $V_j(z)$ obtained through the Volterra scattering inverse series in R_k/T_k and the exact barrier. Square barrier test case: $V_0 = -3.0$, $a = 0.5$.

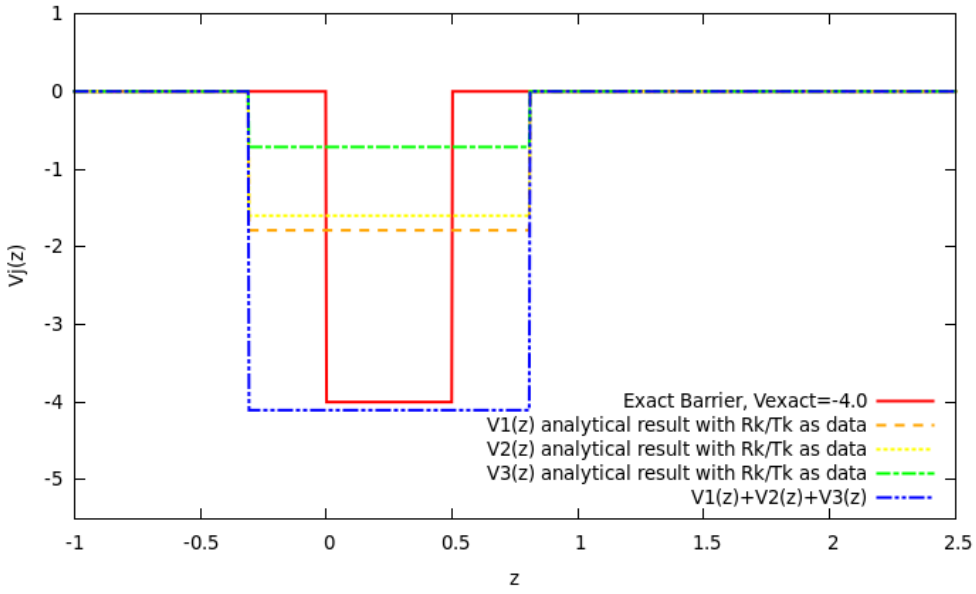

Figure 3.5. Comparison of $V_j(z)$ obtained through the Volterra inverse scattering series in R_k/T_k and the exact barrier. Square barrier test case: $V_0 = -4.0$, $a = 0.5$.

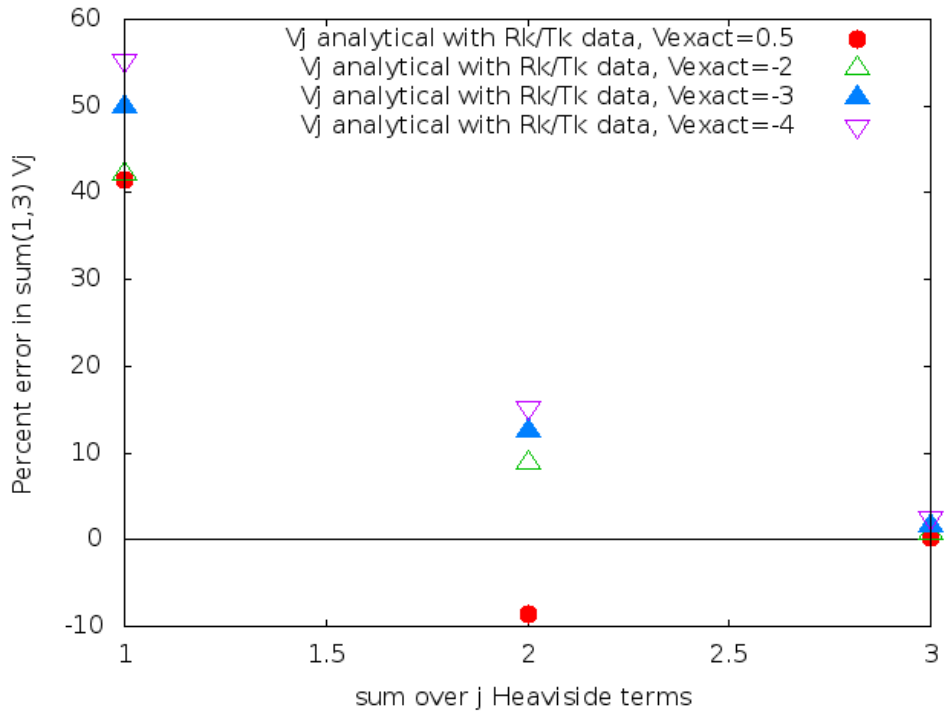

Figure 3.6. Error in % for $\sum_j V_j(z)$ obtained through the Volterra inverse scattering series in R_k/T_k for different values of V_0 of the square barrier test case.

Table 3.1. Amplitude error in function of the number of V_j terms correction.

V_0	$A(V_1)$	$A(V_2)$	$A(V_3)$	Error $V_1(\%)$	Error $\sum_{i=1}^{2} V_i(\%)$	Error $\sum_{i=1}^{3} V_i(\%)$
0.5	0.707	-0.25	0.044	41.4	8.6	0.2
-2.0	-1.155	-0.667	-0.192	42.25	8.95	0.7
-3.0	-1.500	-1.125	-0.422	50	12.5	1.57
-4.0	-1.789	-1.600	-0.716	55.275	15.275	2.6

3.2.2 Depth correction

The errors in the depth (onset of the barrier or well and end of the barrier or well) are symmetrical when one uses R_k/T_k data. In the case of a barrier, the height of the first term $|A(V_1)|$ and thus $c(z)$ are overestimated. The barrier width is smaller than the exact one, since the corrected term is for a P-wave travelling faster than it should. In the case of a well, the height of the first term $|A(V_1)|$ and thus $c(z)$ is underestimated. It results into the predicted well width to be wider. As mentioned in [25] for the square barrier, the Dirac-δ function and its higher derivatives are associated with a Taylor expansion of Heaviside functions which correct the error in the depth. As shown in Figures 3.2, 3.3, 3.4, the Heaviside terms of the first three orders of Volterra inverse scattering series with R_k/T_k series show excellent convergence to the exact amplitude. The correction on the depth comes from the Dirac-δ function and its derivative terms, as explained by Weglein[25]. This can be demonstrated by using the expansion of the Heaviside function as a Taylor series.

The Taylor series for a Heaviside function $f(z) = \eta(z - z_0)$ expanded about $\widehat{z}_0$ can be written as:

$$\begin{aligned} f(z) &= \eta(z - z_0) = \sum_{n=0}^{\infty} \frac{(z_0 - \widehat{z}_0)^n}{n!} \frac{\partial^n f(z)}{\partial z^n}|_{z=\widehat{z}_0} \\ &= \eta(z - \widehat{z}_0) + \delta(z - \widehat{z}_0)(z_0 - \widehat{z}_0) + \delta'(z - \widehat{z}_0)\frac{(z_0 - \widehat{z}_0)^2}{2} + O[(z_0 - \widehat{z}_0)^3]. \end{aligned} \tag{3.14}$$

On the left hand side of the inverse series results, we write the correction between the incorrectly-placed Heaviside and the correct Heaviside function:

$$C_{left}(z) = V_0(\eta(z_1 - z) - \eta(z_0 - z)) = -V_0(\eta(z_0 - z) - \eta(z_1 - z)), \quad (3.15)$$

with $z_0 = 0$ the exact depth. Its Taylor series around z_1 is given by:

$$C_{left}(z) = -V_0[\delta(z - z_1)(z_1 - z_0) + \delta'(z - z_1)\frac{(z_1 - z_0)^2}{2} + O((z_0 - \widehat{z}_0)^3)]. \quad (3.16)$$

From

$$z_1 = \frac{a}{2}(1 - \sqrt{1 - V_0}), \quad (3.17)$$

$$z_2 = \frac{a}{2}(1 + \sqrt{1 - V_0}), \quad (3.18)$$

we obtain

$$z_1 - z_0 = \frac{z_2 - z_1}{2}(\frac{1}{\sqrt{1 - V_0}} - 1). \quad (3.19)$$

Then we find an expression for the exact coefficients of the Taylor series correction in $\delta^n(z - z_1)$ truncated at the second order:

$$\begin{aligned} C_{left}(z) &= -V_0[\delta(z - z_1)\frac{z_2 - z_1}{2}(\frac{1}{\sqrt{1 - V_0}} - 1) \\ &+ \delta'(z - z_1)\frac{(z_2 - z_1)^2}{8}(\frac{1}{\sqrt{1 - V_0}} - 1)^2 + O((z_2 - z_1)^3)]. \end{aligned} \quad (3.20)$$

In table 3.2, we compare the exact $\delta(z - z_1)$ coefficient and the coefficients that come from terms V_2 and V_3. In table 3.3, for the cases of last section, we evaluate the $\delta(z - z_1)$ coefficients.

In table 3.4, we compare the exact $\delta'(z - z_1)$ coefficient and the coefficients that

Table 3.2. Comparison of $\delta(z - z_1)$ coefficients.

The exact	From V_2	From $V_2 + V_3$
$V_0\frac{z_2 - z_1}{2}(\frac{1}{\sqrt{1-V_0}} - 1)$	$\frac{V_0^2}{4(1-V_0)}(z_2 - z_1)$	$\frac{V_0^2}{4(1-V_0)}(z_2 - z_1) - \frac{1}{16}(z_2 - z_1)(\frac{V_0}{\sqrt{1-V_0}})^3$

Table 3.3. Comparison of $\delta(z-z_1)$ coefficients for each case

V_0	a	The exact	From V_2	Error(%)	From V_2+V_3	Error(%)
0.5	1	0.0732	0.0884	20.77	0.0728	0.55
-2	0.5	0.366	0.2887	21.12	0.372	1.64
-3	0.5	0.75	0.5625	25	0.74734	3.12
-4	0.5	1.2361	0.8944	27.64	1.2944	4.72

Table 3.4. Comparison of $\delta'(z-z_1)$ coefficients in each case

The exact	From V_3
$-\frac{(z_2-z_1)^2}{8}(\frac{1}{\sqrt{1-V_0}}-1)^2$	$-\frac{1}{32}(z_2-z_1)^2(\frac{V_0}{\sqrt{1-V_0}})^3$

Table 3.5. Comparison of $\delta'(z-z_1)$ coefficients for each case

V_0	a	The exact	From V_3	Error(%)
0.5	1	-0.0054	-0.0055	1.85
-2	0.5	0.0335	0.0361	7.76
-3	0.5	0.0938	0.1055	12.47
-4	0.5	0.1910	0.2236	17.07

come from the V_3 term. In table 3.5, for different cases we discussed above, we evaluate the $\delta'(z-z_1)$ coefficients.

From the analysis above, we find that the Dirac-δ function and its derivative terms perform the task of depth correction. For low velocity contrast, the differences of the coefficients between the exact Dirac-δ function and its derivative terms and the series result are rather small, which means that we can obtain a reasonably accurate depth with only few orders. The same values of the δ and δ' coefficients result for the correction of the right side since the width error is symmetrical.

Combining these analyses, we find that the Volterra inverse scattering series with R_k/T_k converges nicely to the exact interaction. For low velocity contrast, the Volterra inverse series shows excellent convergence with only few terms. For high velocity contrast, we probably need to evaluate some higher order terms to obtain the desired accuracy.

3.3 RESULTS FOR VISS WITH R_k

Using the Volterra inverse scattering series with R_k as the sole data (Eq.(2.38)), we obtain the results for the first two orders for the square well or barrier (The details of computation are given in appendix D),

$$\begin{aligned}
V_1(z) &= 4\sum_{j=0}^{\infty}\left(\frac{1-\sqrt{1-V_0}}{\sqrt{1-V_0}+1}\right)^{2j+1}\eta(z-ja\sqrt{1-V_0})\eta[(j+1)a\sqrt{1-V_0}-z], \\
V_2(z) &= -\sum_{j=0}^{\infty}8\left(\frac{1-\sqrt{1-V_0}}{\sqrt{1-V_0}+1}\right)^{4j+2}\eta(z-jz_1)\eta[(j+1)z_1-z] \\
&+ \sum_{j=0}^{\infty}\sum_{m=0}^{j-1}8z_1\left(\frac{1-\sqrt{1-V_0}}{\sqrt{1-V_0}+1}\right)^{2(j+m+1)}[\delta[(j+1)z_1-z]-\delta(z-jz_1)] \\
&+ \sum_{j=0}^{\infty}8z_1\left(\frac{1-\sqrt{1-V_0}}{\sqrt{1-V_0}+1}\right)^{4j+2)}\delta[(j+1)z_1-z]. \qquad (3.21)
\end{aligned}$$

Since the analytical computation of the Volterra inverse scattering series is complicated, we only carry out calculations up to the second order. In addition, we evaluated the portion of $V_3(z)$ generated by the Heaviside corrections. Our sub-series is:

$$\begin{aligned}
V_3'(z) &= \sum_{n=0}^{\infty}\frac{C_n^3}{8}\eta(z-nz_1)\eta[(n+1)z_1-z] \\
&+ \sum_{j=0}^{\infty}\sum_{n=0}^{\infty}\frac{C_j^2C_n}{16}[\eta(z-nz_1)\eta[(n+1)z_1-z]-\eta[z-(n+1)z_1]\eta[(n+2)z_1-z] \\
&- \sum_{j=1}^{\infty}\sum_{m=0}^{j-1}\sum_{n=0}^{\infty}C_jC_mC_n[\eta[z-(n+j-m-1)z_1]\eta[(n+j-m-1)z_1-z] \\
&\quad +\eta[z-(n+j-m+1)z_1]\eta[(n+j-m+2)z_1-z] \\
&\quad -2\eta[z-(n+j-m)z_1]\eta[(n+j-m+1)z_1-z]. \qquad (3.22)
\end{aligned}$$

For different values of V_0 (cf Figures 3.7, 3.8, 3.9 and 3.10), we compare the plots of the exact barrier, and the first three order $V_j(z)$ obtained through the Volterra inverse series with only the R_k data. As previously for the Volterra inverse scattering series with R_k/T_k, we sum up only the Heaviside contributions and not the derivatives of the Dirac-δ function. Figure 3.11 shows the height convergence as a function of the number of summed V_j higher

order terms. Table 3.6 shows the amplitude error as a function of the number of V_j terms included.

We can observe that the Volterra inverse scattering series with R_k converges more

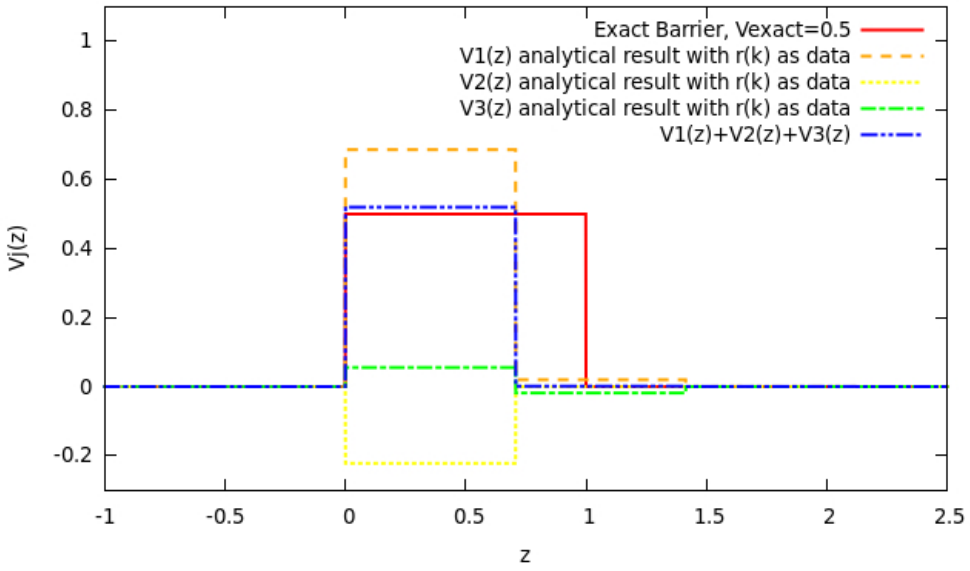

Figure 3.7. Comparison of $V_j(z)$ obtained through the Volterra inverse scattering series in R_k and the exact barrier. Square barrier test case: $V_0 = 0.5$, $a = 1.0$.

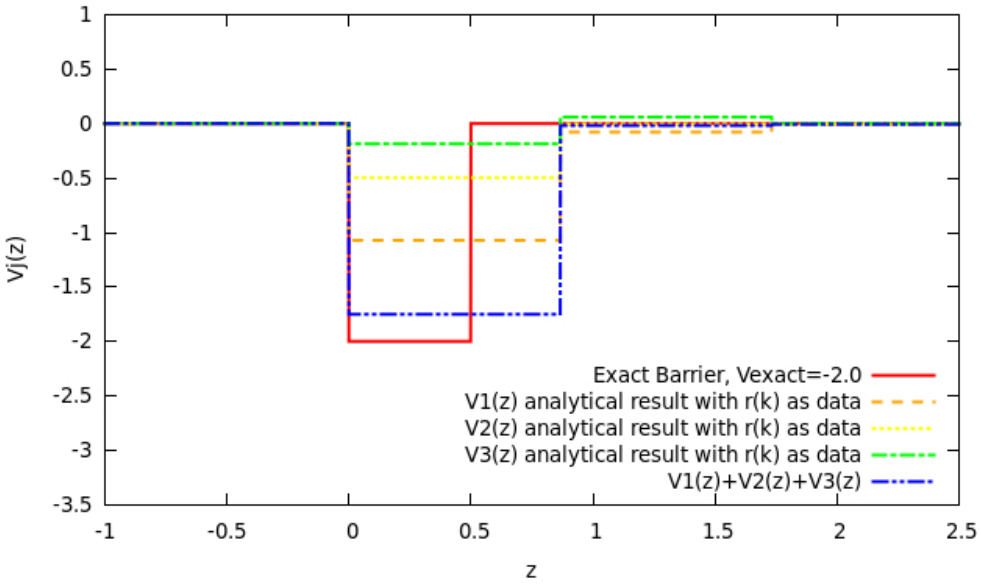

Figure 3.8. Comparison of $V_j(z)$ obtained through the Volterra inverse scattering series in R_k and the exact barrier. Square barrier test case: $V_0 = -2.0$, $a = 0.5$.

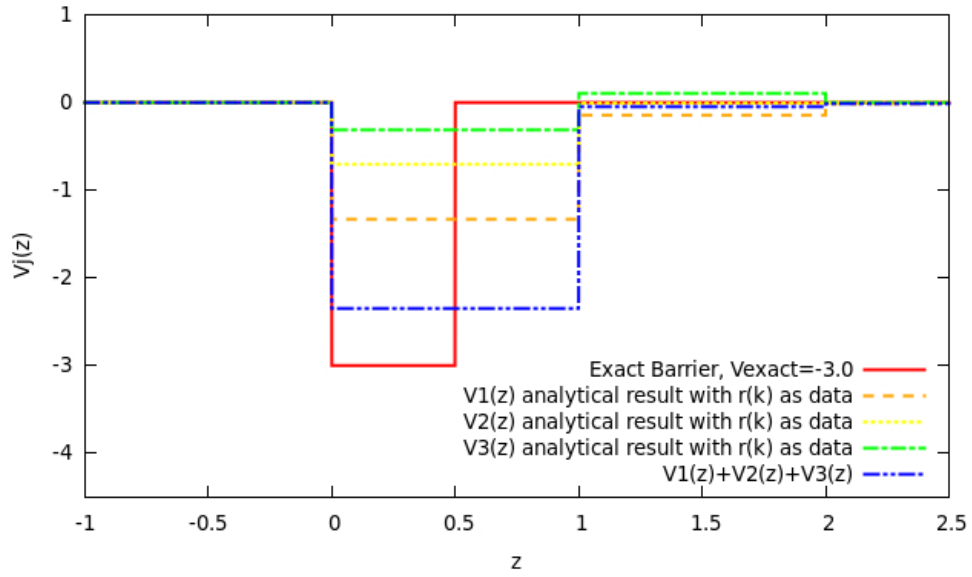

Figure 3.9. Comparison of $V_j(z)$ obtained through the Volterra inverse scattering series in R_k and the exact barrier. Square barrier test case: $V_0 = -3.0$, $a = 0.5$.

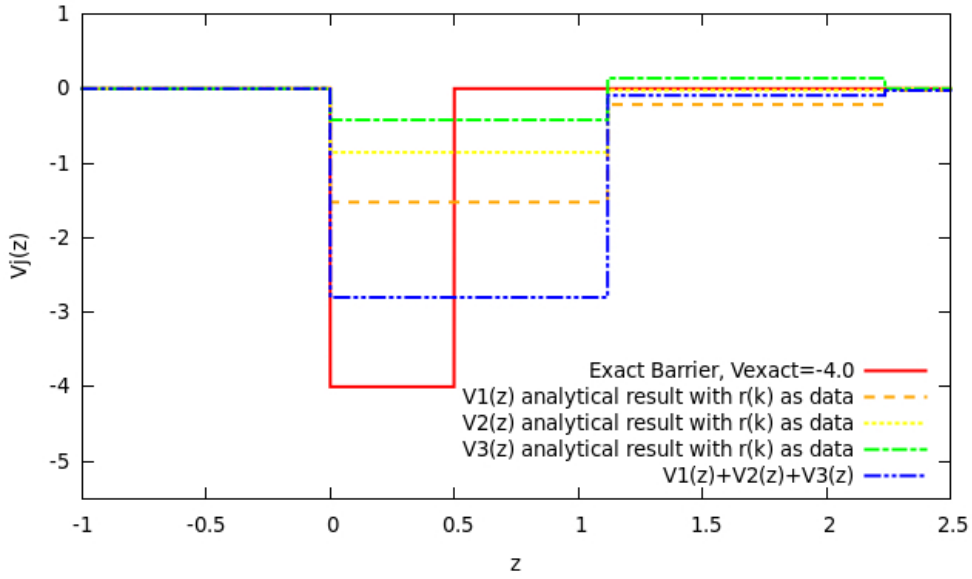

Figure 3.10. Comparison of $V_j(z)$ obtained through the Volterra inverse scattering series in R_k and the exact barrier. Square barrier test case: $V_0 = -4.0$, $a = 0.5$.

slowly than the VISS with R_k/T_k data. For VISS with R_k, we conclude that higher orders are needed to attain higher levels of accuracy.

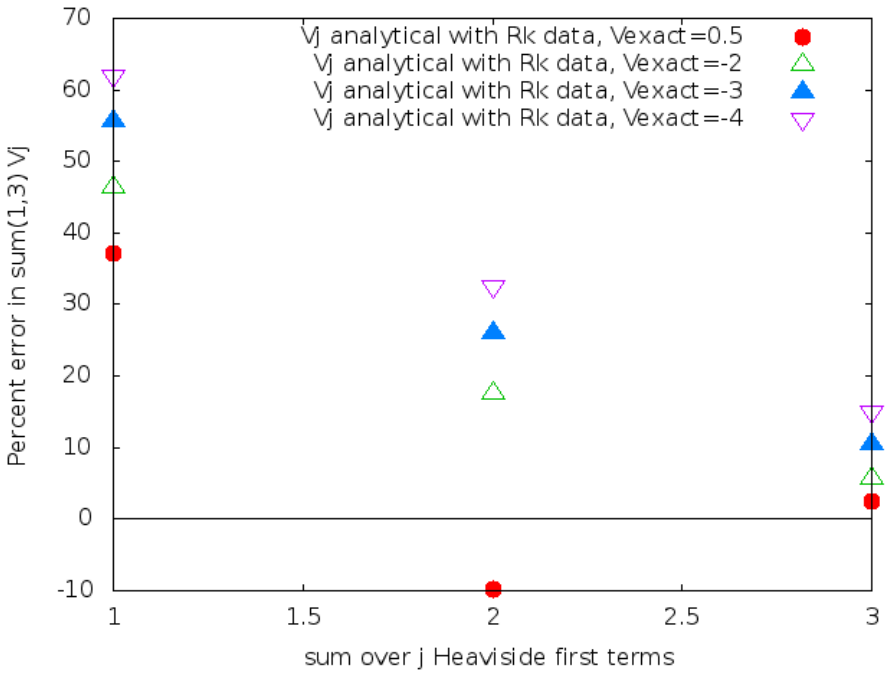

Figure 3.11. Error in % for $\sum_j V_j(z)$ obtained through the Volterra inverse scattering series in R_k for different values of V_0 of the square barrier test case.

Table 3.6. Amplitude error in function of the number of V_j terms correction.

V_0	$A(V_1)$	$A(V_2)$	$A(V_3)$	Error $V_1(\%)$	Error $\sum_{i=1}^{2} V_i(\%)$	Error $\sum_{i=1}^{3} V_i(\%)$
0.5	0.686	-0.235	0.061	37.2	9.8	2.4
-2.0	-1.072	-0.574	-0.237	46.4	17.7	5.8
-3.0	-1.33	-0.889	-0.463	55.6	26	10.5
-4.0	-1.523	-1.167	-0.707	61.9	32.6	15

CHAPTER 4 THE APPLICATION OF VOLTERRA INVERSE SCATTERING SERIES TO THE GAUSSIAN INTERACTION

The Volterra inverse scattering series has been introduced and has been applied analytically for several exact square barrier or well velocity models. We find that even with three orders, the results are very encouraging. The next step is to develop a numerical algorithm to deal with more realistic conditions with the ultimate objective of developing it into an algorithm ready for application to field data. In this chapter, we report tests of our Volterra inverse scattering series for a Gaussian velocity interaction:

$$V(z) = V_0 e^{-\frac{(z-a)^2}{b^2}}. \tag{4.1}$$

Thus, this interaction yields

$$c(z) = \sqrt{\frac{c_0^2}{V_0 e^{-\frac{(z-a)^2}{b^2}} - 1}}. \tag{4.2}$$

This chapter is organised as follows: first, in order to get scattering data, we develop an algorithm to generate the reflection and transmission data of the Gaussian interaction based on Volterra renormalization of Lippmann-Schwinger equation; then we numerically evaluate the results of Volterra inverse scattering series of Gaussian interaction with both the reflection and transmission data and with using only the reflection data.

4.1 FORWARD SCATTERING ALGORITHM BASED ON VOLTERRA RENORMALIZATION OF THE LIPPMANN-SCHWINGER EQUATION

4.1.1 The derivation of the forward scattering algorithm

Before getting started with the inverse scattering, it is necessary for us to generate scattering data by solving the forward scattering problem. Instead of solving the Helmholtz

equation Eq.(2.1) with specified boundary conditions, we carry out an algorithm to solve for the pressure wave based on Volterra renormalization of Lippmann-Schwinger equation (Eq.(2.26)[16],

$$\begin{aligned} P_k^+(z) &= e^{ikz} + R_k e^{-ikz} + \int_{-\infty}^{\infty} dz' \widetilde{G}_{0k}(z,z') V(z') P_k^+(z') \\ &= e^{ikz} + R_k e^{-ikz} + k \int_{-\infty}^{z} dz' k \sin[k(z-z')] V(z') P_k^+(z'). \end{aligned} \tag{4.3}$$

As stated in Chapter 2, we can assume the solution of the above equation takes the following form:

$$P_k^+(z) = P_{1k}(z) + R_k P_{2k}(z), \tag{4.4}$$

which gives:

$$\begin{aligned} P_{1k}(z) &= e^{ikz} + \int_{-\infty}^{z} dz' \widetilde{G}_{0k}(z,z') V(z') P_{1k}(z') \\ &= e^{ikz} + k \int_{-\infty}^{z} dz' \sin[k(z-z')] V(z') P_{1k}(z'), \end{aligned} \tag{4.5}$$

$$P_{2k}(z) = P_{1k}^*(z). \tag{4.6}$$

From Eq.(2.6), we can also get that

$$\begin{aligned} R_k &= -\frac{ik}{2} \int_{-\infty}^{\infty} e^{ikz'} V(z') P_k^+(z') \\ &= -\frac{ik}{2} \int_{-\infty}^{\infty} e^{ikz'} V(z') [P_{1k}(z) + R_k P_{1k}^*(z)]. \end{aligned} \tag{4.7}$$

Rearranging the above equation, we can get R_k

$$R_k = \frac{-\frac{ik}{2} \int_{-\infty}^{\infty} dz' e^{ikz'} V(z') P_{1k}(z')}{1 + \frac{ik}{2} \int_{-\infty}^{\infty} dz' e^{ikz'} V(z') P_{1k}^*(z')}. \tag{4.8}$$

Furthermore, we can also get the expression for T_k with Eq.(2.7):

$$\begin{aligned} T_k &= 1 - \frac{ik}{2} \int_{-\infty}^{\infty} e^{-ikz'} V(z') P_k^+(z') \\ &= 1 - \frac{ik}{2} \int_{-\infty}^{\infty} e^{-ikz'} V(z') [P_{1k}(z) + R_k P_{1k}^*(z)] \\ &= 1 - \frac{ik}{2} \int_{-\infty}^{\infty} e^{-ikz'} V(z') P_{1k}(z) - \frac{ik}{2} R_k \int_{-\infty}^{\infty} e^{-ikz'} V(z') P_{1k}^*(z). \end{aligned} \tag{4.9}$$

By directly solving Eq.(4.4)-(4.5), we can obtain value of R_k and T_k by numerical integration of Eqs. (4.7) and (4.8). The following is a detailed description of the numerical procedure [26].

Algorithm

Comment[Define computational grid.]

Assume that the velocity interaction is compactly supported, which means that it is nonzero only within a finite region $[z_1, z_2]$. For an interaction that does not have compact support, we can choose z_1, z_2 so that $V(z)$ is small enough for $z < z_1, z > z_2$ to neglect it for those values of z. Then create n subintervals on $[z_1, z_2]$ by choosing a set of points $b_0, b_1, \ldots, b_j, \ldots, b_n$, with $b_0 = z_1, b_j = z_1 + j\Delta, b_n = z_2$.

Step 1

Comment [Construct the numerical solution for P_{1k}, P_{2k} of Eq.(4.4) on each grid node b_j.]
(1) Compute the value of P_{1k} at each node.
For $j = 0$

$$P_{1k}(b_0) \;=\; e^{ikz_1}. \tag{4.10}$$

Do $j = 1, 2, \ldots, n$

$$\begin{aligned} P_{1k}(b_j) &= e^{ik(z_1+j\Delta)} + k\int_{z_1}^{z_1+j\Delta} dz' \sin[k(z_1+\Delta-z')]V(z')P_{1k}(z') \\ &= e^{ik(z_1+\Delta)} + k\Delta\sum_{l=1}^{j-1} \sin[k(j-l)\Delta]V_1(z_1+l\Delta)P_{1k}(z_1+l\Delta),\ j = 1:n. \end{aligned} \tag{4.11}$$

End Do

(2) From Eq.(A.4), we can generate the result of P_{2k} since it is the complex conjugate of P_{1k}.

Step 2

Comment [Construct the numerical solution for R_k of Eq.(A.6) on each grid node b_j.]

(1) Evaluate the first integral $I_1 = \int_{z_1}^{z_2} dz' e^{ikz'} V(z') P_{1k}(z')$ in Eq.(A.6).

Do $j = 0, 1, 2, \ldots, n-1$

$$\begin{aligned} I_1 &= I_1 + \frac{\Delta}{2}[e^{ik(z_1+j\Delta)} V(z_1 + j\Delta) P_{1k}(z_1 + j\Delta) \\ &\quad + e^{ikz_1+(j+1)\Delta} V(z_1 + (j+1)\Delta) P_{1k}(z_1 + (j+1)\Delta). \end{aligned} \tag{4.12}$$

End Do

(2) Evaluate the second integral $I_2 = \int_{-\infty}^{\infty} dz' e^{ikz'} V(z') P_{1k}^*(z')$ in Eq.(A.6) with the same algorithm.

(3) Using Eq. (A.6) to compute the value of R_k.

Step 3

Comment [Construct the numerical solution for T_k of Eq.(A.7) on each grid node b_j.as step 2.]

(1) Evaluate the first integral $I_3 = \int_{-\infty}^{\infty} e^{-ikz'} V(z') P_{1k}(z)$ in Eq.(A.7)with trapezoidal rule.

(2) Evaluate the second integral $I_4 = \int_{-\infty}^{\infty} e^{-ikz'} V(z') P_{1k}^*(z)$ in Eq.(A.7) with the same algorithm.

(3) Compute the solution of T_k.

Step 4

Comment [Compute the numerical solution for P_k with Eq.(A.2)]

Evaluate the P_k at each node.

Do $j = 0, 1, 2, \ldots, n$

$$P_k(b_j) = P_{1k}(b_j) + R_k P_{2k}(b_j). \tag{4.13}$$

End Do

Note: The algorithm introduced above uses complex arithmetic.

4.1.2 The numerical results

We tested the algorithm for the type of the Gaussian velocity interaction (as shown in Figure 4.1). The reflection and transmission data are shown in figures 4.2 and figure 4.3

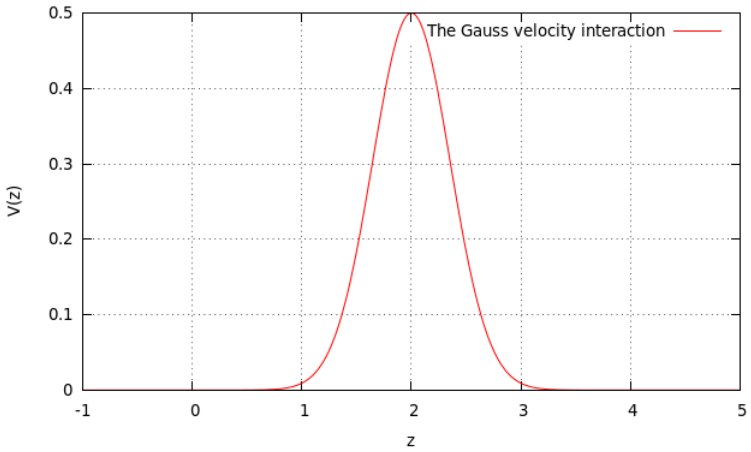

Figure 4.1. The Gaussian interaction with $V_0 = 0.5, a = 2, b = 1/2$

separately.

4.2 THE NUMERICAL RESULTS OF VISS FOR THE GAUSSIAN INTERACTION

4.2.1 The numerical result of the Volterra inverse scattering series with R_k/T_k for the Gaussian interaction

Based on the inverse scattering series introduced in Chapter 2, we can numerically evaluate the result of each order $V_j, j = 1, 2, 3, \cdots$ for the Gaussian velocity interaction. Figure 4.4 shows the results for the first three orders of Gaussian velocity contrast with amplitude parameters that correspond to barrier obtained through the Volterra inverse scattering series with R_k/T_k data. For this barrier model, the velocity $c(z)$ is greater than the reference velocity, c_0. The Volterra inverse scattering series is observed to converge

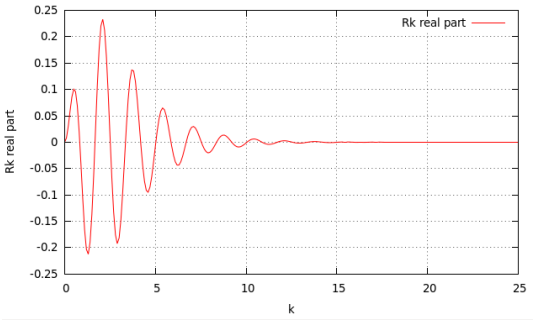

(a) The real part of R_k

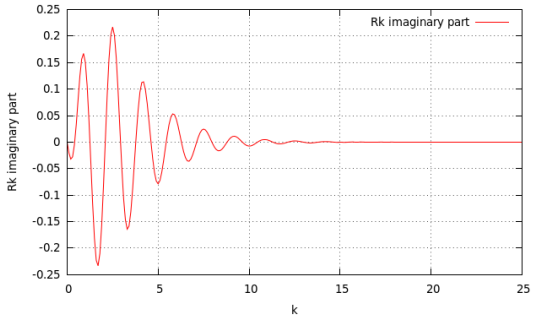

(b) The imaginary part of R_k

Figure 4.2. The reflection data for the Gaussian interaction with $V_0 = 0.5, a = 2, b = 1/2$: (a) the real part of T_k; (b) the imaginary part of R_k.

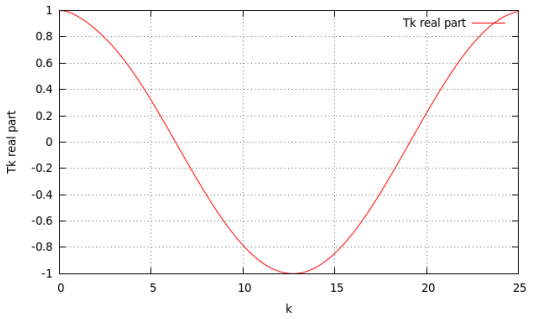

(a) The real part of T_k

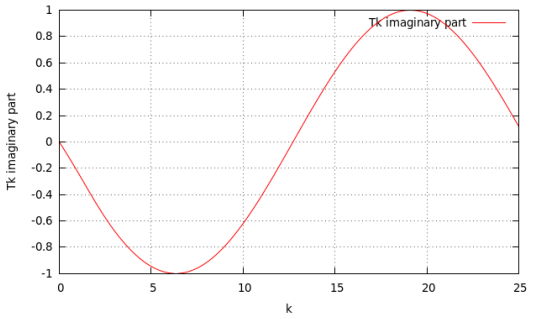

(b) The imaginary part of T_k

Figure 4.3. The transmission data for the Gaussian interaction with $V_0 = 0.5, a = 2, b = 1/2$: (a) The real part of T_k; (b) the imaginary part of T_k.

rapidly to the true velocity interaction. The amplitudes of the higher order terms are seen to diminish gradually. In figure 4.5, the exact interaction and cumulative sums of these first three orders are displayed. Table 4.1 shows the corresponding L^2-distance between the exact Gaussian velocity contrast and the cumulative sums of the first three orders[1]. We can observe that the exact Gaussian interaction and the sum of the first three orders are quite similar. After only three terms, the mis-estimation of the velocity has been corrected. Summing more terms in the Volterra inverse scattering series for this example is not necessary.

[1]The L^2-distance between two function $f(x)$ and $g(x)$ is $\|f-g\|_2 = \sqrt{\int_a^b |f(x)-g(x)|^2 dx}$

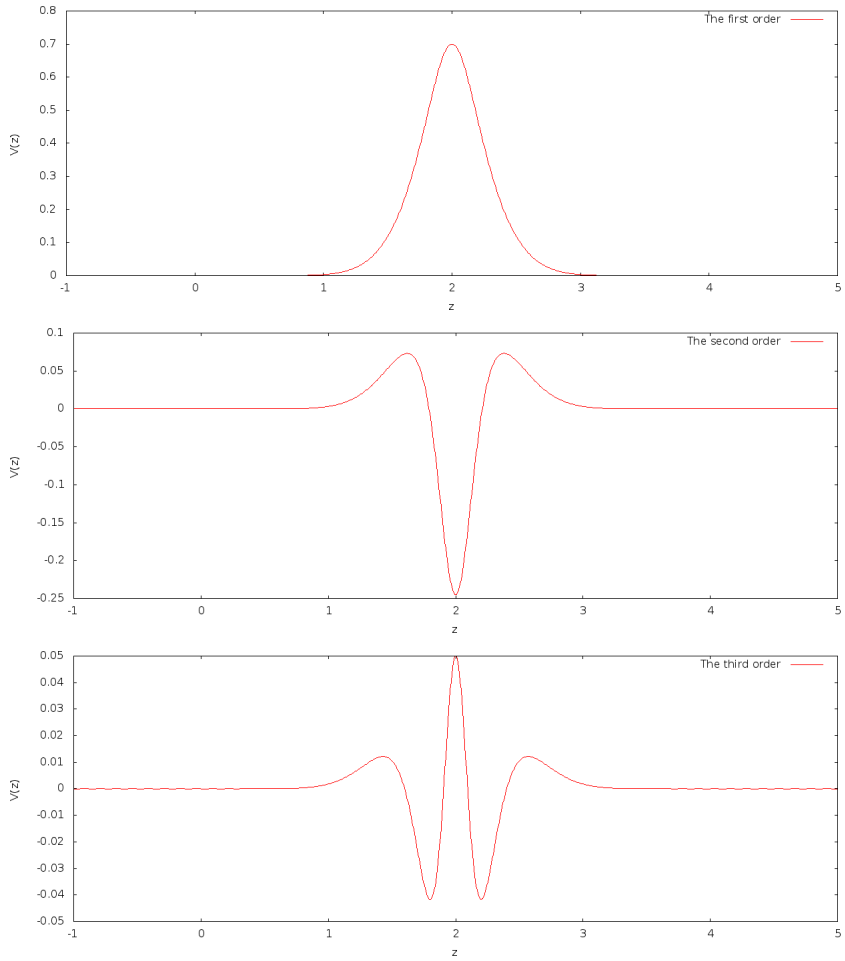

Figure 4.4. The first three order of VIIS with R_k/T_k for the Gaussian interaction with $V_0 = 0.5, a = 2, b = 1/2$: (a) the first order; (b) the second order; (c) the third order.

Figures 4.6 illustrates the results of the Gaussian interaction with amplitude param-

Table 4.1. The L^2-distance in terms of V_j terms correction of Gaussian barrier

Orders included	V_1	$\sum_{j=1}^{2} V_j$	$\sum_{j=1}^{3} V_j$
L^2-distance	0.2710	0.0674	0.0194

eters that correspond to well (the velocity $c(z)$ is lower than the reference velocity, c_0). As we can observe, when the velocity contrast is relatively large, it may not be sufficiently accurate just to evaluate the first three orders. Higher orders of the Volterra inverse scattering series can be included to obtain more accurate results. Figure 4.7 shows the results of the

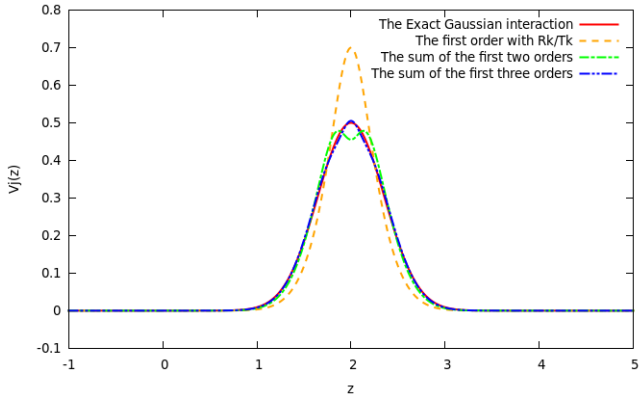

Figure 4.5. The comparison of the exact Gaussian interaction and the cumulative sums of the first three order result of VIIS with R_k/T_k:$V_0 = 0.5, a = 2, b = 1/2$

fourth order and the comparison of the exact interaction and the sum of the first four orders. As we can see from the figures, the VISS result converges to the exact result excellently after including the fourth order. Table 4.2 shows the corresponding L^2-distance between the exact Gaussian velocity contrast and the cumulative sums of the first four orders.

Table 4.2. The L^2-distance in terms of V_j terms correction of Gaussian well

Orders included	V_1	$\sum_{j=1}^{2} V_j$	$\sum_{j=1}^{3} V_j$	$\sum_{j=1}^{4} V_j$
L^2-distance	0.2709	0.0806	0.0329	0.0148

4.2.2 The numerical results of the Volterra inverse scattering series with R_k for the Gaussian interaction

Similar to VISS with R_k/T_k, we can also get the Volterra inverse scattering series results for a Gauss interaction using only reflection data. Figure 4.8 shows the results of the first four orders of Gaussian velocity interaction with amplitude parameter that correspond to barrier obtained through the Volterra inverse scattering series with R_k. The amplitudes of the higher order terms are also seen to diminish gradually. In figure 4.9, the exact barrier interaction and the cumulative sums of the first four orders are displayed. We observe

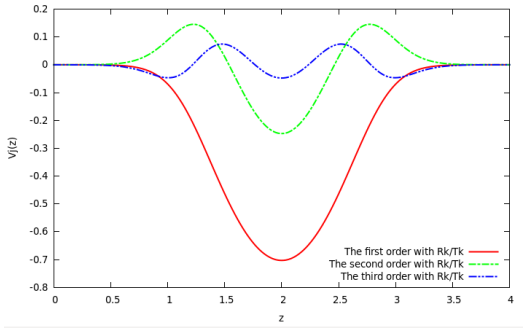

(a) The first three order

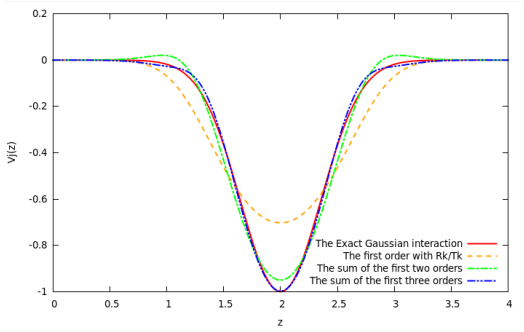

(b) The exact result and the sum of the first three orders

Figure 4.6. The VISS result with R_k/T_k of the Gaussian interaction with $V_0 = -1, a = 2, b = 1/2$

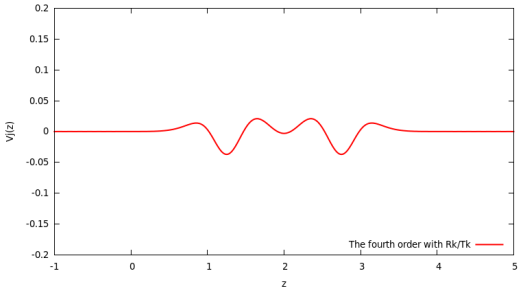

(a) The fourth order

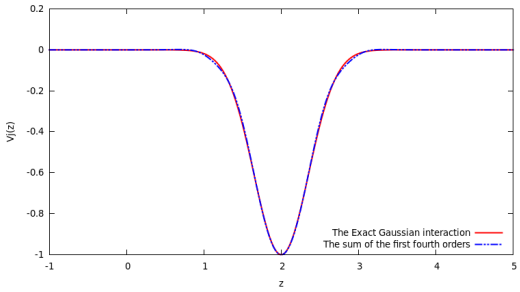

(b) The exact result and the sum of the first four orders

Figure 4.7. The VISS fourth order result with R_k/T_k of the Gaussian interaction with $V_0 = -1, a = 2, b = 1/2$

that the sum of the first four orders converges to the true Gaussian interaction. Figure 4.10 illustrate the results for the Gaussian well interaction through the Volterra inverse scattering series with R_k. Table 4.3 shows the L^2-distance between the exact Gaussian velocity contrast and the cumulative sums of the first four orders for this two models. Although the error between the exact Gaussian volecity interaction and the results of VISS with R_k for large velocity contrast cannot be neglected, it becomes smaller and smaller after summing more higher order terms. The tests of Gaussian interaction also shows that the VISS with R_k/T_k converges faster than VISS with R_k. For the same velocity interaction, it

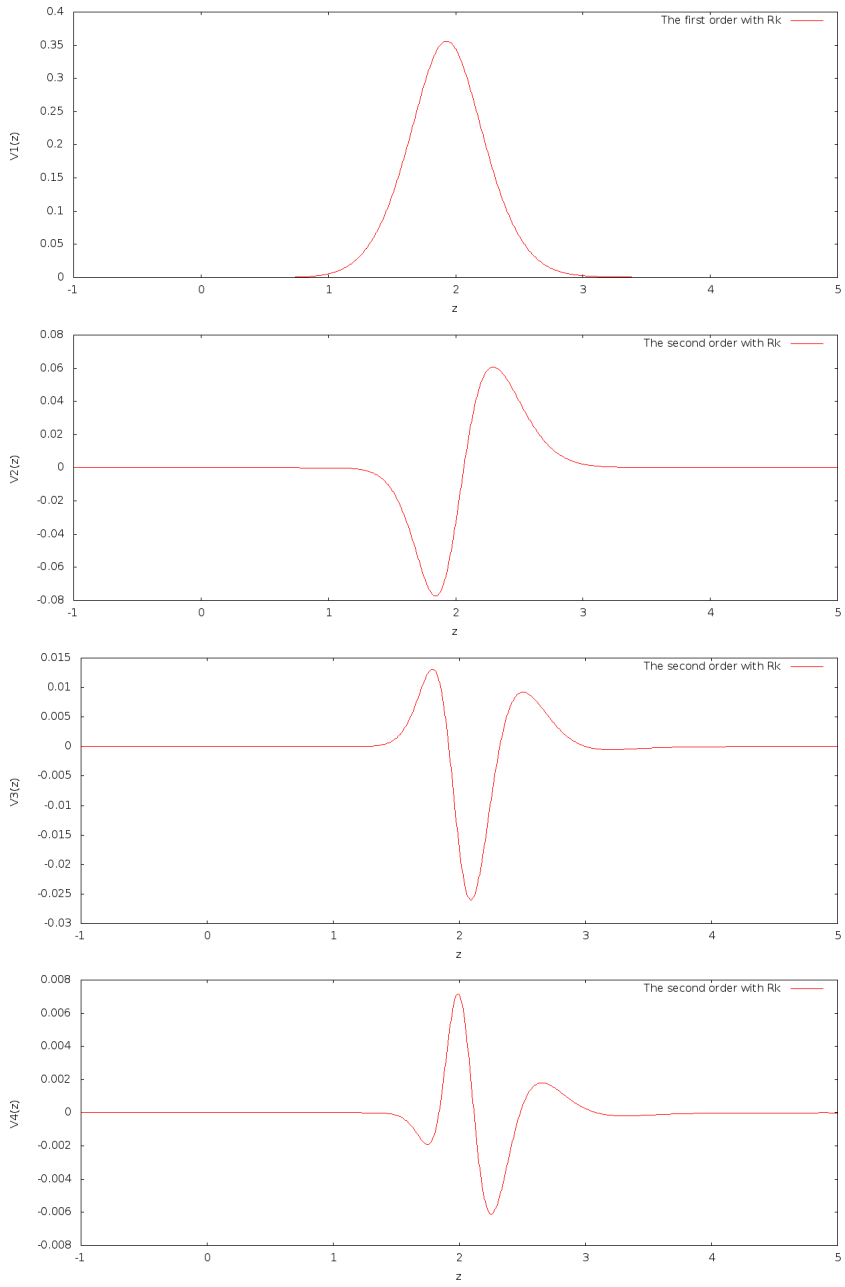

Figure 4.8. The first four orders of VIIS with R_k for the Gaussian interaction with $V_0 = 0.3, a = 2, b = 1/2$: (a) the first order; (b) the second order; (c) the third order; (d) the fourth order.

might need to carry out more high order terms for VISS with R_k to obtain the same degree of accuracy.

Table 4.3. The L^2-distance in terms of V_j terms correction for VISS with R_k

V_0	V_1	$\sum_{j=1}^{2} V_j$	$\sum_{j=1}^{3} V_j$	$\sum_{j=1}^{4} V_j$
0.3	0.2078	0.0535	0.0151	0.0045
-1	0.3920	0.1955	0.1229	0.0861

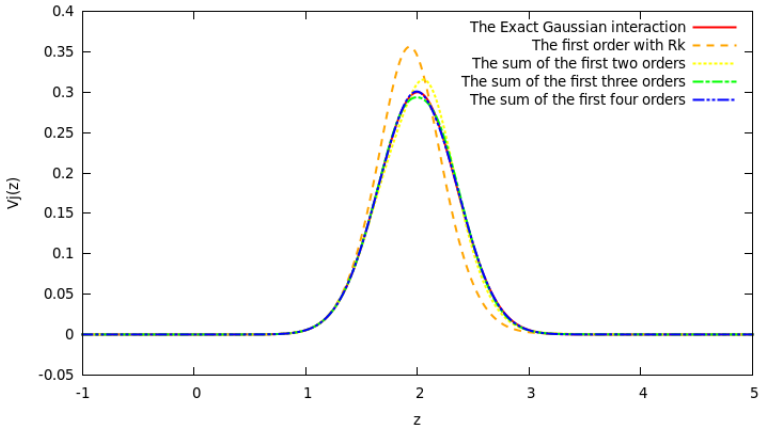

Figure 4.9. The comparison of the exact Gaussian interaction and the cumulative sums of the first four ordere result of VIIS with R_k:$V_0 = 0.5, a = 2, b = 1/2$

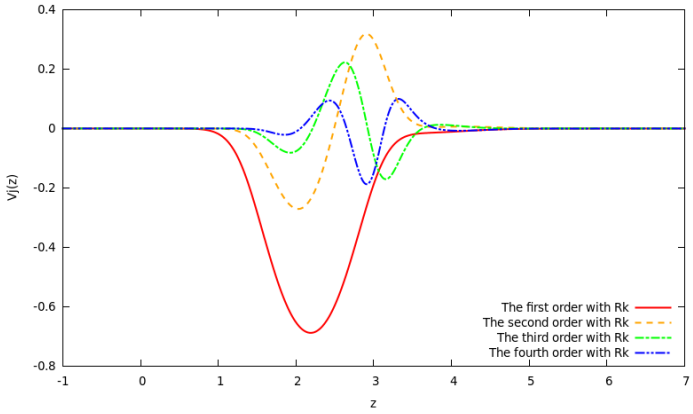

(a) The first fourth order

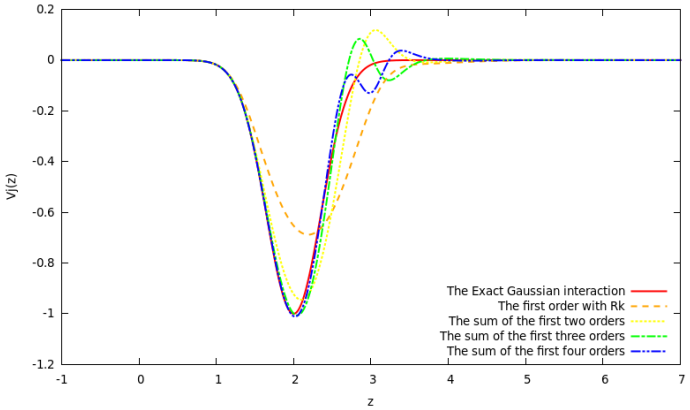

(b) The exact result and the sum of the first fourth order

Figure 4.10. The VISS result with $R_k$of the Gaussian interaction with $V_0 = -1, a = 2, b = 1/2$

CHAPTER 5 CONCLUSION

5.1 SUMMARY OF THE THESIS

The research in this thesis represents several fundamental advances in the Volterra inverse scattering series approach. As stated by Weglein, the inverse scattering series represents a unique opportunity to achieve all processing objectives without knowing, or iteratively determining the actual velocity governing wave propagation in the subsurface. The thesis demonstrates progress in the extension of the inverse acoustic scattering series approach presented in Kouri and Vijay [5]. First, higher order contributions for two velocity interactions have been obtained using R_k/T_k as the input data. Second, the approach has been generalized to apply when one only has reflection data. The approach consists in combining two ideas: the renormalization of the Lippmann-Schwinger equation to obtain a Volterra equation framework and the formal series expansion using reflection coefficients. As proved in this thesis, the renormalization method possesses the best possible convergence behavior under Born-Neumann iteration. Here the square barriers and wells and Gaussian interactions have been studied. The results demonstrate that the Volterra inverse scattering series method is an effective tool in inverse scattering. The results are shown to benefit from having both reflection and transmission data, in that the series converges to the true velocity interaction faster than if the transmission data is absent. In addition, we have shown that a Volterra-based inversion can be done as a single comprehensive task, without separating task-specified subseries.

5.2 FUTURE WORK

In the future, further analysis of the 1-D Volterra inverse scattering series will be continued, including testing on more realistic media, studying the effects of the lower frequency data, analysis of higher orders of VISS and influence of noise on the inversion. In

addition, we will derive the Volterra inverse scattering series for two and three dimensions. We will apply it to solve full dimensional acoustic data, including field data. Finally, we will explore extending the theory beyond the acoustic case to include elastic scattering.

REFERENCES

[1] R. Jost and W. Kohn, "Construction of a potential from a phase shift," *Phys. Rev.*, vol. 87, pp. 977–992, Sep 1952.

[2] H. E. Moses, "Calculation of the scattering potential from reflection coefficients," *Phys. Rev.*, vol. 102, pp. 559–567, Apr 1956.

[3] M. Razavy, "Determination of the wave velocity in an inhomogeneous medium from the reflection coefficient," *J. Acoust. Soc. Am.*, vol. 58, p. 956, Jun 1956.

[4] R. T. Prosser, "Formal solutions of inverse scattering problems," *Journal of Mathematical Physics*, vol. 10, no. 10, pp. 1819–1822, 1969.

[5] D. J. Kouri and A. Vijay, "Inverse scattering theory: Renormalization of the lippmann-schwinger equation for acoustic scattering in one dimension," *Phys. Rev. E*, vol. 67, p. 046614, Apr 2003.

[6] A. B. Weglein, F. V. Araĺšjo, P. M. Carvalho, R. H. Stolt, K. H. Matson, R. T. Coates, D. Corrigan, D. J. Foster, S. A. Shaw, and H. Zhang, "Inverse scattering series and seismic exploration," *Inverse Problems*, vol. 19, no. 6, p. R27, 2003.

[7] J. K. Cohen and N. Bleistein, "An inverse method for determining small variations in propagation speed," *SIAM Journal on Applied Mathematics*, vol. 32, no. 4, pp. pp. 784–799, 1977.

[8] R. Stolt, "Migration by fourier transform," *GEOPHYSICS*, vol. 43, no. 1, pp. 23–48, 1978.

[9] R. Stolt and A. Weglein, "Migration and inversion of seismic data," *GEOPHYSICS*, vol. 50, no. 12, pp. 2458–2472, 1985.

[10] A. Weglein, F. Gasparotto, P. Carvalho, and R. Stolt, "An inverse scattering series method for attenuating multiples in seismic reflection data," *GEOPHYSICS*, vol. 62, no. 6, pp. 1975–1989, 1997.

[11] A. B. Weglein, K. H. Matson, and D. J. Foster, "Imaging and inversion at depth without a velocity model: theory, concepts and initial evaluation," *SEG Expanded Abstracts*, 2000.

[12] S. A. Shaw, "An inverse scattering series algorithm for depth imaging of reflection data from a layered acoustic medium with an unknown velocity model," 2005.

[13] F. Liu and U. of Houston, *Multi-dimensional Depth Imaging Without an Adequate Velocity Model*. University of Houston, 2006.

[14] A. Tarantola, "Inversion of seismic reflection data in the acoustic approximation," *Geophysics*, vol. 49, pp. 1259–1266, 1984.

[15] R. G. Pratt, "Seismic waveform inversion in the frequency domain, part 1: Theory and verification in a physical scale model," *Geophysics*, vol. 66, pp. 888–901, 1999.

[16] W. N. Sams and D. J. Kouri, "Noniterative solutions of integral equations for scattering. i. single channels," *The Journal of Chemical Physics*, vol. 51, no. 11, pp. 4809–4814, 1969.

[17] D. Ferry, *Quantum Mechanics: An Introduction for Device Physicists and Electrical Engineers, Second Edition*. Taylor & Francis, 2010.

[18] R. G. Newton, *Scattering theory of waves and particles*. Springer-Verlag, New York, 1982.

[19] R. T. Prosser, "Formal solutions of inverse scattering problems. ii," *Journal of Mathematical Physics*, vol. 17, no. 10, pp. 1775–1779, 1976.

[20] R. T. Prosser, "Formal solutions of inverse scattering problems. iii.," *Journal of Mathematical Physics*, vol. 21, no. 11, pp. 2648–2653, 1980.

[21] R. T. Prosser, "Formal solutions of inverse scattering problems. iv. error estimates," *Journal of Mathematical Physics*, vol. 23, no. 11, pp. 2127–2130, 1982.

[22] L. Rodberg and R. Thaler, *The Quantum Theory of Scattering (Academic Press*. Academic PressNew York, 1967.

[23] J. H. Eberly, "Quantum scattering theory in one dimension," *American Journal of Physics*, vol. 33, no. 10, pp. 771–773, 1965.

[24] S. McMurry, *Quantum mechanics*. Pearson Education, Addison-Wesley, 1994.

[25] A. B. Weglein and S. F., "An inverse-scattering sub-series for predicting the spatial location of reflectors without the precise reference medium and wave velocity," *SEG Expanded Abstracts*, 2001.

[26] W. Tribbey, "Numerical recipes: The art of scientific computing (3rd edition)," *SIGSOFT Softw. Eng. Notes*, vol. 35, pp. 30–31, Nov. 2010.

[27] J. Mathews and R. Walker, *Mathematical Methods of Physics*. Benjamin, New York, 1965.

APPENDIX A CONVERGENCE OF THE FREDHOLM SERIES FOR P_k BASED ON THE VOLTERRA INTEGRAL EQUATION

In this appendix, we give more details regarding the Fredholm solution of Eq.(2.13)

$$P_k^+(z) = T_k e^{ikz} + \gamma \int_z^\infty dz' K(z,z') P_k^+(z'), \tag{A.1}$$

where $K(z,z')$ is defined in Eq.(2.42). The unique solution of the above equation may be written as

$$P_k^+(z) = T_k e^{ikz} + \gamma \int_0^\infty dz' R(z,z';\gamma) T_k e^{ikz'}. \tag{A.2}$$

The resolvent kernel $R(z,z';\gamma)$ can be written as the quotient of the entire functions $D(z,z';\gamma)$ and $D(\gamma)$ given by the series expansions

$$R(z,z';\gamma) = \frac{D(z,z';\gamma)}{D(\gamma)}, \tag{A.3}$$

where the Fredholm minor $D(z,z';\gamma)$ and Fredholm determinant $D(\gamma)$ can be expressed as

$$D(z,z';\gamma) = \sum_{n=0}^{\infty} \frac{(-1)^n}{n!} B_n(z,z') \gamma^n, \tag{A.4}$$

$$D(\gamma) = \sum_{n=0}^{\infty} \frac{(-1)^n}{n!} c_n \gamma^n. \tag{A.5}$$

We can make use of the following recurrence relation to calculate $B_n(z,z')$,c_n .

In the series, $B_0(z,z') = K(z,z')$, and $c_0 = 1$. For every $n \geq 1$, $B_n(z,z')$ can be computed for the recursive relationship

$$B_n(z,z') = c_n K(z,z') - n \int_0^\infty K(z,z'') B_{n-1}(z'',z') dz'', \tag{A.6}$$

and c_n can be computed by evaluating the integral

$$c_n = \int_a^b B_{n-1}(z',z') dz'. \tag{A.7}$$

We can also express the Fredholm determinant $D(\lambda)$ as the trace of the kernel

$$D(\gamma) = \sum_{n=0}^{\infty} TrK^n(-\gamma)^n, \tag{A.8}$$

where the trace is given by

$$TrK = \int_a^b K(z,z)dz, \tag{A.9}$$

and

$$\begin{aligned} TrK^2 &= \frac{1}{2!}\int_0^\infty \int_0^\infty dzdz'[K(z,z)K(z',z') - K(z,z')K(z',z)] \\ &= \frac{1}{2!}\int_0^\infty \int_0^\infty dzdz' \det \begin{pmatrix} K(z,z) & K(z,z') \\ K(z',z) & K(z',z') \end{pmatrix}, \end{aligned} \tag{A.10}$$

or in general

$$TrK^n = \frac{1}{n!}\int_0^\infty \cdots \int_0^\infty \det K(z_i,z_j)|_{1\le i,j\le n} dz_1 \cdots dz_n, \tag{A.11}$$

where

$$K(z_i,z_j) = \begin{pmatrix} K(z_1,z_1) & K(z_1,z_2) & \dots & K(z_1,z_n) \\ K(z_2,z_1) & K(z_2,z_2) & \dots & K(z_2,z_n) \\ \vdots & \vdots & \ddots & \vdots \\ K(z_n,z_1) & K(z_n,z_2) & \dots & K(z_n,z_n) \end{pmatrix}. \tag{A.12}$$

Note that $K(z,z)$ vanishes as long as $V(z)$ is not too singular. Therefore, we have $TrK^n = 0$ for $n \ge 1$. Consequently, the Fredholm determinant $D \equiv 1$. Now consider the Fredholm minor. Similarly, the coefficient function $B_n(z,z')$ can also be written as multiple integrals of a determinant. Specifically, for $n \ge 1$, we can have

$$B_n(z,z') = \int_0^\infty \cdots \int_0^\infty dz_1 \dots dz_n \det \Delta_n(z,z'), \tag{A.13}$$

where

$$\Delta_n(z,z') = \begin{pmatrix} K(z,z') & K(z,z_1) & \dots & K(z,z_n) \\ K(z_1,z') & K(z_1,z_1) & \dots & K(z_1,z_n) \\ \vdots & \vdots & \ddots & \vdots \\ K(z_n,z') & K(z_n,z_1) & \dots & K(z_n,z_n) \end{pmatrix}. \tag{A.14}$$

We can estimate the magnitude of the coefficients $B_n(z,z')$ with Hadamard theorems, that states that the absolute value of the determinant of a matrix is less than or equal to the product of the norms of its rows. More precisely, if $\mathbf{A} = (a_{ij})$ is an $n \times n$ matrix and $\mathbf{a}_i = (a_{i1}, \ldots, a_{in})$ is its ith row, them

$$|det\mathbf{A}| \leq \prod_{i=1}^{n} \|\mathbf{a}_i\|, \tag{A.15}$$

where$\|\mathbf{a}_i\| = \sqrt{(a_{i1}^2 + \ldots + a_{in}^2)}$.

As usual in the scattering theory, we assume the potential has compact support on the domain $[z_1, z_2]$, and that it is bounded. Thus, for any value of k and γ,, we can conclude that the kernel$|K(z,z')| < M$, where M is some finite positive number. By Hadamard's inequality, we have that

$$|B_n(z,z')| \leq n^{n/2} M^n (z_2 - z_1)^n. \tag{A.16}$$

Then, the coefficient of γ^n in Eq.(B.4) is bounded by $n^{n/2}/n! M^n (z_2 - z_1)^n$. Since $n^n/n! < e^n$, then the nth root of this coefficient is less that$M(z_2 - z_1)e/n^{1/2}$, which vanishes as $n \to \infty$. Hence the power series for the Fredholm minor $D(z,z';\gamma)$ converges independent of the strength of the coupling parameter γ or the value of k.

We can also show that when the Fredholm determinant equals 1, the Fredholm solution is identical to the Born-Neumann iterative solution of the integral equation[27].It is obvious that $c_n = 0$ for $n \geq 1$, so we have:

$$\begin{aligned} B_n(z,z') &= -n \int_0^\infty K(z,z'') B_{n-1}(z'',z') dz'' \\ &= (-1)^n n! \int_0^\infty \cdots \int_0^\infty dz_1 \ldots dz_n K(z,z_1) K(z_1,z_2) \ldots K(z_j,z_{j+1}) \ldots K(z_n,z'). \end{aligned} \tag{A.17}$$

Combing Eq.(A.2), (A.4) and (A.17), we can get

$$\begin{aligned} P_k^+(z) &= T_k e^{ikz} + \sum_{n=1}^{\infty} \gamma^n \int_0^\infty \cdots \int_0^\infty dz_1 \ldots dz_n \\ &\times K(z,z_1) K(z_1,z_2) \ldots K(z_j,z_{j+1}) \ldots K(z_n,z') T_k e^{ikz'}. \end{aligned} \tag{A.18}$$

In abstract form, this is

$$P_k^+(z) \;=\; T_k \sum_{n=0}^{\infty} K^n |k>, \tag{A.19}$$

which is identical to the Born-Neumann iterative solution.

APPENDIX B COMPUTATION OF THE FIRST THREE ORDERS FOR THE SQUARE WELL OR BARRIER INTERACTION WITH R_k/T_k

The reflection and transmission coefficients of the square well or barrier are given as follows:

$$R_k = \frac{V_0 \sin(ak\sqrt{1-V_0})}{(2-V_0)\sin(ak\sqrt{1-V_0}) + 2i\sqrt{1-V_0}\cos(ak\sqrt{1-V_0})}, \tag{B.1}$$

$$T_k = \frac{2\sqrt{1-V_0}e^{-ika}}{V_0 \sin(ka\sqrt{1-V_0})}R_k. \tag{B.2}$$

B.1 THE FIRST ORDER

From the first order of VISS with R_k/T_k, we can have

$$V_1(2k) = \frac{2iR_k}{kT_k} = \frac{V_0}{k\sqrt{1-V_0}} sin(ka\sqrt{1-V_0})e^{ika}. \tag{B.3}$$

We can get the expression for $V_1(z)$ by inverse fourier transform of $V_1(2k)$

$$V_1(z) = \frac{V_0}{\pi\sqrt{1-V_0}} \int_{-\infty}^{\infty} dk \frac{sin(ka\sqrt{1-V_0})}{k} e^{ik(a-2z)}, \tag{B.4}$$

which is recognized as the Fourier transform of the sinc function. Then we can obtain the the first order result:

$$V_1(z) = \frac{V_0}{\pi\sqrt{1-V_0}} \eta(z-z_1)\eta(z_2-z), \tag{B.5}$$

where $z_1 = \frac{a}{2}(1-\sqrt{1-V_0})$,$z_2 = \frac{a}{2}(1+\sqrt{1-V_0})$

B.2 THE SECOND ORDER

From Eq.(2.22), we have

$$V_2(2k) = - < -k|V_1 \widetilde{G}_{0k} V_1|k > . \tag{B.6}$$

Substituting the Green's function and the result of the first order, we have

$$\begin{aligned}
V_2(2k) &= - < -k|V_1\widetilde{G}_{0k}V_1|k > \\
&= -\int_{-\infty}^{\infty} dz' \int_{-\infty}^{\infty} dz'' e^{ik(z'+z'')} V_1(z')\widetilde{G}_{0k}V_1(z'') \\
&= -\frac{V_0^2 k}{1-V_0}\int_{z_1}^{z_2} dz' \int_{z_1}^{z'} dz'' e^{ik(z'+z'')}\frac{e^{ik(z'-z'')} - e^{-ik(z'-z'')}}{2i} \\
&= -\frac{V_0^2 k}{1-V_0}\int_{z_1}^{z_2} dz' \int_{z_1}^{z'} dz'' e^{ik(z'+z'')}\frac{e^{ik(z'-z'')} - e^{-ik(z'-z'')}}{2i} \\
&= \frac{iV_0^2 k}{2(1-V_0)}\int_{z_1}^{z_2} dz' \int_{z_1}^{z'} dz''(e^{2ikz'} - e^{2ikz''}) \\
&= \frac{iV_0^2 k}{2(1-V_0)}\int_{z_1}^{z_2} dz' e^{2ikz'} \int_{z_1}^{z'} dz'' - \frac{iV_0^2 k}{2(1-V_0)}\int_{z_1}^{z_2} dz' \int_{z_1}^{z'} dz'' e^{2ikz''} \\
&= \frac{iV_0^2 k}{2(1-V_0)}\int_{z_1}^{z_2} dz' e^{2ikz'}(z'-z_1) - \frac{iV_0^2 k}{2(1-V_0)}\int_{z_1}^{z_2} dz' \int_{z_1}^{z'} dz'' e^{2ikz''} \\
&= \frac{V_0^2}{1-V_0}[\frac{e^{2ikz_2} + e^{2ikz_1}}{4}(z_2-z_1) + \frac{i}{4k}(e^{2ikz_2} - e^{2ikz_1})]. \qquad \text{(B.7)}
\end{aligned}$$

Then, we find

$$\begin{aligned}
V_2(z) &= \frac{1}{\pi}\int_{-\infty}^{\infty} dk V_2(2k) e^{-2ikz} \\
&= \frac{V_0^2}{\pi(1-V_0)}\int_{-\infty}^{\infty} dk[\frac{e^{2ik(z_2-z)} + e^{2ik(z_1-z)}}{4}(z_2-z_1) \\
&\quad + \frac{i}{4k}(e^{2ik(z_2-z)} - e^{2ik(z_1-z)})] \\
&= \frac{V_0^2(z_2-z_1)}{\pi(1-V_0)}[\frac{\pi\delta(z_1-z)}{4} + \frac{\pi\delta(z_2-z)}{4}] \\
&= -\frac{V_0^2}{2(1-V_0)}\eta(z-z_1)\eta(z_2-z) \\
&\quad + \frac{V_0^2}{4(1-V_0)}(z_2-z_1)[\delta(z_1-z) + \delta(z_2-z)].
\end{aligned}$$

(B.8)

B.3 THE THIRD ORDER

From Eq.(2.23), we have the series expression for the third order

$$\begin{aligned} V_3(2k) &= - < -k|V_2\widetilde{G}_{0k}V_1|k > - < -k|V_1\widetilde{G}_{0k}V_2|k > \\ &\quad - < -k|V_1\widetilde{G}_{0k}V_1\widetilde{G}_{0k}V_1|k > . \end{aligned} \tag{B.9}$$

The first two terms are mathematically analogous to Eq.(B.7) in the derivation of $V_2(2k)$. The integral equation for the first term is:

$$\begin{aligned} V_3^1(2k) &= - < -k|V_2GV_1|k > \\ &= - \int_{-\infty}^{\infty} dz' \int_{-\infty}^{\infty} dz'' e^{ik(z'+z'')} V_2(z') k \sin[k(z'-z'')] \eta(z'-z'') V_1(z'') \\ &= \frac{ik}{2} \int_{-\infty}^{\infty} dz' \int_{-\infty}^{z'} dz'' (e^{2ikz'} - e^{2ikz''}) V_2(z') V_1(z'') \\ &= \frac{ik}{2} \int_{-\infty}^{\infty} dz' \int_{-\infty}^{z'} dz'' (e^{2ikz'} - e^{2ikz''}) \\ &\times [-\frac{V_0^2}{2(1-V_0)} \eta(z'-z_1)\eta(z_2-z')][\frac{V_0}{\sqrt{1-V_0}} \eta(z''-z_1)\eta(z_2-z'')] \\ &+ \frac{ik}{2} \int_{-\infty}^{\infty} dz' \int_{-\infty}^{z'} dz'' (e^{2ikz'} - e^{2ikz''}) \\ &\times [\frac{V_0^2}{4(1-V_0)} (z_2-z_1)[\delta(z_1-z) + \delta(z_2-z)]] \\ &\times [\frac{V_0}{\sqrt{1-V_0}} \eta(z''-z_1)\eta(z_2-z'')] \\ &= -\frac{ik}{4} (\frac{V_0}{\sqrt{1-V_0}})^3 \int_{z_1}^{z_2} dz' \int_{z_1}^{z'} dz'' (e^{2ikz'} - e^{2ikz''}) \\ &+ \frac{ik}{8} (\frac{V_0}{\sqrt{1-V_0}})^3 (z_2-z_1) \int_{z_1}^{z_2} dz'' (e^{2ikz_1} - e^{2ikz''}) \\ &= -\frac{ik}{4} (\frac{V_0}{\sqrt{1-V_0}})^3 [\frac{e^{2ikz_2} + e^{2ikz_1}}{2ik} (z_2-z_1) + \frac{1}{2k^2} (e^{2ikz_2} - e^{2ikz_1})] \\ &+ \frac{ik}{8} (\frac{V_0}{\sqrt{1-V_0}})^3 (z_2-z_1)[e^{2ikz_2}(z_2-z_1) - \frac{1}{2ik} (e^{2ikz_2} - e^{2ikz_1})] \\ &= -(\frac{V_0}{\sqrt{1-V_0}})^3 [\frac{e^{2ikz_2} + e^{2ikz_1}}{8} (z_2-z_1) + \frac{i}{8k} (e^{2ikz_2} - e^{2ikz_1})] \\ &+ (\frac{V_0}{\sqrt{1-V_0}})^3 (z_2-z_1)[\frac{ik}{8} e^{2ikz_2}(z_2-z_1) - \frac{1}{16} (e^{2ikz_2} - e^{2ikz_1})]. \end{aligned} \tag{B.10}$$

The integral equation for second term is

$$
\begin{aligned}
V_3^2(2k) &= - < -k|V_1 G V_2|k > \\
&= -\int_{-\infty}^{\infty} dz' \int_{-\infty}^{\infty} dz'' e^{ik(z'+z'')} V_1(z') k \sin[k(z'-z'')] \eta(z'-z'') V_2(z'') \\
&= \frac{ik}{2} \int_{-\infty}^{\infty} dz' \int_{-\infty}^{z'} dz'' (e^{2ikz'} - e^{2ikz''}) V_1(z') V_2(z'') \\
&= \frac{ik}{2} \int_{-\infty}^{\infty} dz' \int_{-\infty}^{z'} dz'' (e^{2ikz'} - e^{2ikz''}) \\
&\times [\frac{V_0}{\sqrt{1-V_0}} \eta(z'-z_1)\eta(z_2-z')][-\frac{V_0^2}{2(1-V_0)} \eta(z''-z_1)\eta(z_2-z'')] \\
&+ \frac{ik}{2} \int_{-\infty}^{\infty} dz' \int_{-\infty}^{z'} dz'' (e^{2ikz'} - e^{2ikz''}) \\
&\times [\frac{V_0}{\sqrt{1-V_0}} \eta(z'-z_1)\eta(z_2-z')] \\
&\times [\frac{V_0^2}{4(1-V_0)} (z_2-z_1)[\delta(z_1-z'') + \delta(z_2-z'')]] \\
&= -(\frac{V_0}{\sqrt{1-V_0}})^3 [\frac{e^{2ikz_2} + e^{2ikz_1}}{8}(z_2-z_1) + \frac{i}{8k}(e^{2ikz_2} - e^{2ikz_1})] \\
&- (\frac{V_0}{\sqrt{1-V_0}})^3 (z_2-z_1)[\frac{ik}{8} e^{2ikz_1}(z_2-z_1) - \frac{1}{16}(e^{2ikz_2} - e^{2ikz_1})]. \qquad \text{(B.11)}
\end{aligned}
$$

The integral equation for the third term is

$$
\begin{aligned}
V_3^3(2k) &= - < -k|V_1 G V_1 G V_1|k > \\
&= -\int_{-\infty}^{\infty} dz' \int_{-\infty}^{\infty} dz'' \int_{-\infty}^{\infty} dz''' e^{ik(z'+z''')} V_1(z') G V_1(z'') G V_1(z''') \\
&= \frac{k^2}{4} \int_{-\infty}^{\infty} dz' \int_{-\infty}^{\infty} dz'' \int_{-\infty}^{\infty} dz''' V_1(z') V_1(z'') V_1(z''') \\
&\times (e^{2ikz'} - e^{2ikz''} + e^{2ikz'''} - e^{2ikz'-2ikz''+2ikz'''}) \eta(z'-z'')\eta(z''-z''') \\
&= \frac{k^2}{4} (\frac{V_0}{\sqrt{1-V_0}})^3 \int_{z_1}^{z_2} dz' e^{2ikz'} \int_{z_1}^{z'} dz'' \int_{z_1}^{z''} dz''' \\
&- \frac{k^2}{4} (\frac{V_0}{\sqrt{1-V_0}})^3 \int_{z_1}^{z_2} dz' \int_{z_1}^{z'} dz'' e^{2ikz''} \int_{z_1}^{z''} dz''' \\
&+ \frac{k^2}{4} (\frac{V_0}{\sqrt{1-V_0}})^3 \int_{z_1}^{z_2} dz' \int_{z_1}^{z'} dz'' \int_{z_1}^{z''} dz''' e^{2ikz'''} \\
&- \frac{k^2}{4} (\frac{V_0}{\sqrt{1-V_0}})^3 \int_{z_1}^{z_2} dz' e^{-2ikz'} \int_{z_1}^{z'} dz'' e^{2ikz''} \int_{z_1}^{z''} dz''' e^{2ikz'''}. \qquad \text{(B.12)}
\end{aligned}
$$

For the first integral of the third term is

$$\begin{aligned}
&\frac{k^2}{4}(\frac{V_0}{\sqrt{1-V_0}})^3 \int_{z_1}^{z_2} dz' e^{2ikz'} \int_{z_1}^{z'} dz'' \int_{z_1}^{z''} dz''' \\
&= \frac{k^2}{4}(\frac{V_0}{\sqrt{1-V_0}})^3 \int_{z_1}^{z_2} dz' e^{2ikz'} \int_{z_1}^{z'} dz''(z''-z_1) \\
&= \frac{k^2}{4}(\frac{V_0}{\sqrt{1-V_0}})^3 \int_{z_1}^{z_2} dz' e^{2ikz'} \frac{(z'-z_1)^2}{2} \\
&= \frac{k^2}{4}(\frac{V_0}{\sqrt{1-V_0}})^3 \frac{1}{2ik}[e^{2ikz'} \frac{(z'-z_1)^2}{2}|_{z_1}^{z_2} - \int_{z_1}^{z_2} dz' e^{2ikz'}(z'-z_1)] \\
&= \frac{k^2}{4}(\frac{V_0}{\sqrt{1-V_0}})^3 \frac{1}{2ik}[e^{2ikz_2} \frac{(z_2-z_1)^2}{2} - \frac{1}{2ik}[e^{2ikz'}(z'-z_1)|_{z_1}^{z_2} - \int_{z_1}^{z_2} dz' e^{2ikz'}]] \\
&= \frac{k^2}{4}(\frac{V_0}{\sqrt{1-V_0}})^3 \frac{1}{2ik}[e^{2ikz_2} \frac{(z_2-z_1)^2}{2} - \frac{1}{2ik}[e^{2ikz_2}(z_2-z_1) - \frac{1}{2ik}(e^{2ikz_2} - e^{2ikz_1})]] \\
&= (\frac{V_0}{\sqrt{1-V_0}})^3[-\frac{ik}{8} e^{2ikz_2} \frac{(z_2-z_1)^2}{2} + \frac{1}{16} e^{2ikz_2}(z_2-z_1) - \frac{1}{32ik}(e^{2ikz_2} - e^{2ikz_1}).
\end{aligned} \tag{B.13}$$

The second integral

$$\begin{aligned}
&-\frac{k^2}{4}(\frac{V_0}{\sqrt{1-V_0}})^3 \int_{z_1}^{z_2} dz' \int_{z_1}^{z'} dz'' e^{2ikz''} \int_{z_1}^{z''} dz''' \\
&= \frac{1}{16}(\frac{V_0}{\sqrt{1-V_0}})^3 (e^{2ikz_1} + e^{2ikz_2})(z_2-z_1) - \frac{1}{16ik}(\frac{V_0}{\sqrt{1-V_0}})^3 (e^{2ikz_2} - e^{2ikz_1}).
\end{aligned} \tag{B.14}$$

The third integral

$$\begin{aligned}
&\frac{k^2}{4}(\frac{V_0}{\sqrt{1-V_0}})^3 \int_{z_1}^{z_2} dz' e^{2ikz'} \int_{z_1}^{z'} dz'' \int_{z_1}^{z''} dz''' e^{2ikz'''} \\
&= (\frac{V_0}{\sqrt{1-V_0}})^3[\frac{ik}{8} e^{2ikz_1} \frac{(z_2-z_1)^2}{2} + \frac{1}{16} e^{2ikz_1}(z_2-z_1) - \frac{1}{32ik}(e^{2ikz_2} - e^{2ikz_1})].
\end{aligned} \tag{B.15}$$

The fourth integral

$$\begin{aligned}
&-\frac{k^2}{4}(\frac{V_0}{\sqrt{1-V_0}})^3 \int_{z_1}^{z_2} dz' e^{2ikz'} \int_{z_1}^{z'} dz'' e^{2ikz''} \int_{z_1}^{z''} dz''' e^{2ikz'''} \\
&= \frac{1}{16}(\frac{V_0}{\sqrt{1-V_0}})^3 (e^{2ikz_1} + e^{2ikz_2})(z_2-z_1) - \frac{1}{16ik}(\frac{V_0}{\sqrt{1-V_0}})^3 (e^{2ikz_2} - e^{2ikz_1}).
\end{aligned} \tag{B.16}$$

Then

$$
\begin{aligned}
V_3^3(2k) &= - < -k|V_1GV_1GV_1|k > \\
&= -\int_{-\infty}^{\infty} dz' \int_{-\infty}^{\infty} dz'' \int_{-\infty}^{\infty} dz''' e^{ik(z'+z''')} V_1(z')GV_1(z'')GV_1(z''') \\
&= (\frac{V_0}{\sqrt{1-V_0}})^3[-\frac{ik}{8}e^{2ikz_2}\frac{(z_2-z_1)^2}{2} + \frac{1}{16}e^{2ikz_2}(z_2-z_1) - \frac{1}{32ik}(e^{2ikz_2}-e^{2ikz_1}) \\
&+ \frac{1}{16}(\frac{V_0}{\sqrt{1-V_0}})^3(e^{2ikz_1}+e^{2ikz_2})(z_2-z_1) - \frac{1}{16ik}(\frac{V_0}{\sqrt{1-V_0}})^3(e^{2ikz_2}-e^{2ikz_1}) \\
&+ (\frac{V_0}{\sqrt{1-V_0}})^3[+\frac{ik}{8}e^{2ikz_1}\frac{(z_2-z_1)^2}{2} + \frac{1}{16}e^{2ikz_1}(z_2-z_1) - \frac{1}{32ik}(e^{2ikz_2}-e^{2ikz_1})] \\
&+ \frac{1}{16}(\frac{V_0}{\sqrt{1-V_0}})^3(e^{2ikz_1}+e^{2ikz_2})(z_2-z_1) - \frac{1}{16ik}(\frac{V_0}{\sqrt{1-V_0}})^3(e^{2ikz_2}-e^{2ikz_1})] \\
&= (\frac{V_0}{\sqrt{1-V_0}})^3[\frac{3}{16}(e^{2ikz_1}+e^{2ikz_2})(z_2-z_1) - \frac{3}{16ik}(e^{2ikz_2}-e^{2ikz_1}). \\
&\quad -\frac{ik}{16}(e^{2ikz_2}-e^{2ikz_1})(z_2-z_1)^2] \qquad \text{(B.17)}
\end{aligned}
$$

Combining all the terms of the third order:

$$
\begin{aligned}
V_3(2k) &= V_3^1(2k) + V_3^2(2k) + V_3^3(2k) \\
&= -(\frac{V_0}{\sqrt{1-V_0}})^3[\frac{e^{2ikz_2}+e^{2ikz_1}}{8}(z_2-z_1) + \frac{i}{8k}(e^{2ikz_2}-e^{2ikz_1})] \\
&+ (\frac{V_0}{\sqrt{1-V_0}})^3(z_2-z_1)[\frac{ik}{8}e^{2ikz_2}(z_2-z_1) - \frac{1}{16}(e^{2ikz_2}-e^{2ikz_1})] \\
&- (\frac{V_0}{\sqrt{1-V_0}})^3[\frac{e^{2ikz_2}+e^{2ikz_1}}{8}(z_2-z_1) + \frac{i}{8k}(e^{2ikz_2}-e^{2ikz_1})] \\
&- (\frac{V_0}{\sqrt{1-V_0}})^3(z_2-z_1)[\frac{ik}{8}e^{2ikz_1}(z_2-z_1) - \frac{1}{16}(e^{2ikz_2}-e^{2ikz_1})] \\
&+ (\frac{V_0}{\sqrt{1-V_0}})^3[\frac{3}{16}(e^{2ikz_1}+e^{2ikz_2})(z_2-z_1) - \frac{3}{16ik}(e^{2ikz_2}-e^{2ikz_1}) \\
&\quad -\frac{ik}{16}(e^{2ikz_2}-e^{2ikz_1})(z_2-z_1)^2] \\
&= -(\frac{V_0}{\sqrt{1-V_0}})^3[\frac{i}{16k}(e^{2ikz_2}-e^{2ikz_1}) + \frac{e^{2ikz_2}+e^{2ikz_1}}{16}(z_2-z_1) \\
&\quad -\frac{ik}{16}(e^{2ikz_2}-e^{2ikz_1})(z_2-z_1)^2]. \qquad \text{(B.18)}
\end{aligned}
$$

Then, we obtain

$$\begin{aligned} V_3(z) &= \frac{1}{\pi}\int_{-\infty}^{\infty} dk V_3(2k) e^{-2ikz} \\ &= \frac{1}{8}(\frac{V_0}{\sqrt{1-V_0}})^3 \eta(z-z_1)\eta(z_2-z) \\ &- \frac{1}{16}(\frac{V_0}{\sqrt{1-V_0}})^3 (z_2-z_1)[\delta(z_1-z)+\delta(z_2-z)] \\ &+ \frac{1}{32}(\frac{V_0}{\sqrt{1-V_0}})^3 (z_2-z_1)^2[\delta'(z_2-z)-\delta'(z_1-z)]. \end{aligned} \tag{B.19}$$

APPENDIX C COMPUTATION OF THE FIRST THREE ORDERS FOR THE SQUARE WELL OR BARRIER INTERACTION WITH R_k

C.1 THE REFLECTION COEFFICIENT OF SQUARE BARRIER/WELL

The reflection coefficient is given by

$$\begin{aligned} R(k) &= \frac{V_0}{(2-V_0)+2i\sqrt{1-V_0}\cot(ak\sqrt{1-V_0})} \\ &= \frac{V_0\sin(ak\sqrt{1-V_0})}{(2-V_0)\sin(ak\sqrt{1-V_0})+2i\sqrt{1-V_0}\cos(ak\sqrt{1-V_0})} \\ &= \frac{\sin(ak\sqrt{1-V_0})}{\frac{2-V_0}{V_0}\sin(ak\sqrt{1-V_0})+i\frac{2\sqrt{1-V_0}}{V_0}\cos(ak\sqrt{1-V_0})}. \end{aligned} \tag{C.1}$$

The denominator can be simplified as:

$$\begin{aligned} & \frac{2-V_0}{V_0}\sin(ak\sqrt{1-V_0})+i\frac{2\sqrt{1-V_0}}{V_0}\cos(ak\sqrt{1-V_0}) \\ = & \frac{1}{2}[\frac{1-\sqrt{1-V_0}}{1+\sqrt{1-V_0}}+\frac{1+\sqrt{1-V_0}}{1-\sqrt{1-V_0}}]\sin(ak\sqrt{1-V_0}) \\ - & \frac{i}{2}[\frac{1-\sqrt{1-V_0}}{1+\sqrt{1-V_0}}-\frac{1+\sqrt{1-V_0}}{1-\sqrt{1-V_0}}]\cos(ak\sqrt{1-V_0}) \\ = & \frac{e^{\ln\frac{1-\sqrt{1-V_0}}{1+\sqrt{1-V_0}}}+e^{\ln\frac{1+\sqrt{1-V_0}}{1-\sqrt{1-V_0}}}}{2}\sin(ak\sqrt{1-V_0}) \\ + & \frac{e^{\ln\frac{1-\sqrt{1-V_0}}{1+\sqrt{1-V_0}}}-e^{\ln\frac{1+\sqrt{1-V_0}}{1-\sqrt{1-V_0}}}}{2i}\cos(ak\sqrt{1-V_0}). \end{aligned} \tag{C.2}$$

We have the equation of the inverse hyperbolic tangent:

$$\tanh^{-1}(x)=\frac{1}{2}\ln\frac{1+x}{1-x}. \tag{C.3}$$

Using the above equation, we can further simplify the denominator:

$$\begin{aligned}
& \frac{2-V_0}{V_0}\sin(ak\sqrt{1-V_0}) + i\frac{2\sqrt{1-V_0}}{V_0}\cos(ak\sqrt{1-V_0}) \\
= & \frac{e^{-\tanh^{-1}\frac{2\sqrt{1-V_0}}{2-V_0}} + e^{\tanh^{-1}\frac{2\sqrt{1-V_0}}{2-V_0}}}{2}\sin(ak\sqrt{1-V_0}) \\
+ & \frac{e^{-\tanh^{-1}\frac{2\sqrt{1-V_0}}{2-V_0}} - e^{\tanh^{-1}\frac{2\sqrt{1-V_0}}{2-V_0}}}{2i}\cos(ak\sqrt{1-V_0}) \\
= & \frac{1}{2i}[e^{-\tanh^{-1}\frac{2\sqrt{1-V_0}}{2-V_0}}(\cos(ak\sqrt{1-V_0}) + i\sin(ak\sqrt{1-V_0})) \\
- & e^{\tanh^{-1}\frac{2\sqrt{1-V_0}}{2-V_0}}(\cos(ak\sqrt{1-V_0}) - i\sin(ak\sqrt{1-V_0}))] \\
= & \frac{e^{iak\sqrt{1-V_0}-\tanh^{-1}\frac{2\sqrt{1-V_0}}{2-V_0}} - e^{-iak\sqrt{1-V_0}+\tanh^{-1}\frac{2\sqrt{1-V_0}}{2-V_0}}}{2i} \\
= & \sin(ak\sqrt{1-V_0} + i\tanh^{-1}\frac{2\sqrt{1-V_0}}{2-V_0}). \qquad \text{(C.4)}
\end{aligned}$$

The reflection coefficient can then be represented as:

$$R(k) = \frac{\sin(ak\sqrt{1-V_0})}{\sin(ak\sqrt{1-V_0} + i\tanh^{-1}\frac{2\sqrt{1-V_0}}{2-V_0})}. \qquad \text{(C.5)}$$

C.2 THE FIRST ORDER V_1

The first orderV_1 is given by:

$$\begin{aligned}
V_1 &= \frac{2i}{\pi}\int_{-\infty}^{\infty} dk\frac{1}{k}R(k)e^{-2ikz} \\
&= \frac{2i}{\pi}\int_{-\infty}^{\infty} dk\frac{\sin(ak\sqrt{1-V_0})}{k[\sin(ak\sqrt{1-V_0} + i\tanh^{-1}\frac{2\sqrt{1-V_0}}{2-V_0})]}e^{-2ikz}. \qquad \text{(C.6)}
\end{aligned}$$

Simplifying the denominator:

$$\begin{aligned}
& \sin(ak\sqrt{1-V_0} + i\tanh^{-1}\frac{2\sqrt{1-V_0}}{2-V_0}) \\
= & \frac{e^{iak\sqrt{1-V_0}-\tanh^{-1}\frac{2\sqrt{1-V_0}}{2-V_0}} - e^{-iak\sqrt{1-V_0}+\tanh^{-1}\frac{2\sqrt{1-V_0}}{2-V_0}}}{2i} \\
= & \frac{e^{iak\sqrt{1-V_0}}e^{-\tanh^{-1}\frac{2\sqrt{1-V_0}}{2-V_0}} - e^{-iak\sqrt{1-V_0}}e^{\tanh^{-1}\frac{2\sqrt{1-V_0}}{2-V_0}}}{2i} \\
= & \frac{e^{iak\sqrt{1-V_0}}e^{-\ln\frac{\sqrt{1-V_0}+1}{1-\sqrt{1-V_0}}} - e^{-iak\sqrt{1-V_0}}e^{\ln\frac{\sqrt{1-V_0}+1}{1-\sqrt{1-V_0}}}}{2i} \\
= & \frac{e^{iak\sqrt{1-V_0}}\frac{1-\sqrt{1-V_0}}{\sqrt{1-V_0}+1} - e^{-iak\sqrt{1-V_0}}\frac{\sqrt{1-V_0}+1}{1-\sqrt{1-V_0}}}{2i} \\
= & -\frac{e^{-iak\sqrt{1-V_0}}\frac{\sqrt{1-V_0}+1}{1-\sqrt{1-V_0}}}{2i}[1 - e^{2iak\sqrt{1-V_0}}(\frac{1-\sqrt{1-V_0}}{\sqrt{1-V_0}+1})^2].
\end{aligned} \tag{C.7}$$

Then

$$\begin{aligned}
V_1 &= \frac{2i}{\pi}\int_{-\infty}^{\infty} dk \frac{\sin(ak\sqrt{1-V_0})}{k[\sin(ak\sqrt{1-V_0} + \tanh^{-1}\frac{2\sqrt{1-V_0}}{2-V_0})]} e^{-2ikz} \\
&= \frac{4}{\pi}\frac{1-\sqrt{1-V_0}}{\sqrt{1-V_0}+1}\int_{-\infty}^{\infty} dk \frac{\sin(ak\sqrt{1-V_0})e^{-2ikz}}{ke^{-iak\sqrt{1-V_0}}[1 - e^{2iak\sqrt{1-V_0}}(\frac{\sqrt{1-V_0}-1}{\sqrt{1-V_0}+1})^2]} \\
&= \frac{4}{\pi}\frac{1-\sqrt{1-V_0}}{\sqrt{1-V_0}+1}\int_{-\infty}^{\infty} dk \frac{\sin(ak\sqrt{1-V_0})e^{-2ikz+iak\sqrt{1-V_0}}}{k[1 - e^{2iak\sqrt{1-V_0}}(\frac{\sqrt{1-V_0}-1}{\sqrt{1-V_0}+1})^2]}.
\end{aligned} \tag{C.8}$$

The series expansion of $1/(1-x)$ is given by:

$$\frac{1}{1-x} = \sum_0^{\infty} x^n, \tag{C.9}$$

where $|x| < 1$

Using the series expansion for the denominator, we have:

$$\begin{aligned}
V_1 &= \frac{4}{\pi}\frac{1-\sqrt{1-V_0}}{\sqrt{1-V_0}+1}\int_{-\infty}^{\infty} dk \frac{\sin(ak\sqrt{1-V_0})e^{-2ikz+iak\sqrt{1-V_0}}}{k[1-e^{2iak\sqrt{1-V_0}}\frac{\sqrt{1-V_0}-1}{\sqrt{1-V_0}+1}^2]} \\
&= \frac{4}{\pi}\frac{1-\sqrt{1-V_0}}{\sqrt{1-V_0}+1}\int_{-\infty}^{\infty} dk \frac{\sin(ak\sqrt{1-V_0})e^{-2ikz+iak\sqrt{1-V_0}}}{k} \\
&\quad \times \sum_{n=0}^{\infty}(\frac{\sqrt{1-V_0}-1}{\sqrt{1-V_0}+1})^{2n} e^{2niak\sqrt{1-V_0}} \\
&= \sum_{n=0}^{\infty}\frac{4}{\pi}(\frac{1-\sqrt{1-V_0}}{\sqrt{1-V_0}+1})^{2n+1}\int_{-\infty}^{\infty} dk \frac{\sin(ak\sqrt{1-V_0})e^{-2ikz+ia(2n+1)k\sqrt{1-V_0}}}{k} \\
&= 2\sum_{n=0}^{\infty}(\frac{1-\sqrt{1-V_0}}{\sqrt{1-V_0}+1})^{2n+1}[sgn(2(n+1)a\sqrt{1-V_0}-2z) \\
&\quad +sgn(2z-2na\sqrt{1-V_0})] \\
&= 4\sum_{n=0}^{\infty}(\frac{1-\sqrt{1-V_0}}{\sqrt{1-V_0}+1})^{2n+1}\eta(z-na\sqrt{1-V_0})\eta[(n+1)a\sqrt{1-V_0}-z].
\end{aligned} \tag{C.10}$$

C.3 THE SECOND ORDER

Form last section, we know that:

$$V_1 = 4\sum_{n=0}^{\infty}(\frac{1-\sqrt{1-V_0}}{\sqrt{1-V_0}+1})^{2n+1}\eta(z-na\sqrt{1-V_0})\eta[(n+1)a\sqrt{1-V_0}-z]. \tag{C.11}$$

We can write V_1 in the form:

$$V_1 = \sum_{n=0}^{\infty} C_j \eta(z-jz_1)\eta[(j+1)z_1 - z] \ (j = 0, 1, 2, ...), \tag{C.12}$$

where

$$C_j = 4(\frac{1-\sqrt{1-V_0}}{\sqrt{1-V_0}+1})^{2j+1}, \tag{C.13}$$

$$z_1 = a\sqrt{1-V_0}. \tag{C.14}$$

The second order is given by

$$< -k|V_2|k >= - < -k|V_1\widetilde{G}_{0k}V_1|k > - < -k|V_1R_k| - k > . \tag{C.15}$$

C.3.1 The first part of V_2

To calculate $< -k|V_1\widetilde{G}_{0k}V_1|k >$, we can separate it into two terms:$< -k|V_{1j}\widetilde{G}_{0k}V_{1j}|k >$ and $< -k|V_{1j}\widetilde{G}V_{1m}|k > \ (j \neq m)$.

For $< -k|V_{1j}\widetilde{G}_{0k}V_{1j}|k >$, we have

$$\begin{aligned}
< -k|V_{1j}\widetilde{G}V_{1j}|k > &= \int_{-\infty}^{\infty} dz' \int_{-\infty}^{\infty} dz'' e^{ik(z'+z'')} V_{1j}\widetilde{G}_{0k}V_{1j} \\
&= C_j^2 \int_{jz_1}^{(j+1)z_1} dz' \int_{jz_1}^{z'} dz'' e^{ik(z'+z'')} \sin[k(z'-z'')] \\
&= C_j^2 \int_{jz_1}^{(j+1)z_1} dz' \int_{jz_1}^{z'} dz'' e^{ik(z'+z'')} \frac{e^{ik(z'-z'')} - e^{-ik(z'-z'')}}{2i} \\
&= -\frac{iC_j^2 k}{2} \int_{jz_1}^{(j+1)z_1} dz' \int_{jz_1}^{z'} dz'' (e^{2ikz'} - e^{2ikz''}) \\
&= -\frac{iC_j^2 k}{2} [\int_{jz_1}^{(j+1)z_1} dz' e^{2ikz'} \int_{jz_1}^{z'} dz'' - \int_{jz_1}^{(j+1)z_1} dz' \int_{jz_1}^{z'} dz'' e^{2ikz''}].
\end{aligned} \tag{C.16}$$

Then the calculation of the two integrals is given by

$$\int_{jz_1}^{(j+1)z_1} dz' e^{2ikz'} \int_{jz_1}^{z'} dz'' = \frac{e^{2(j+1)ikz_1}}{2ik} z_1 + \frac{1}{4k^2}(e^{2(j+1)ikz_1} - e^{2jikz_1}) \tag{C.17}$$

$$\int_{jz_1}^{(j+1)z_1} dz' \int_{jz_1}^{z'} dz'' e^{2ikz''} = -\frac{1}{4k^2}(e^{2(j+1)ikz_1} - e^{2jikz_1}) - \frac{e^{2jikz_1}}{2ik} z_1. \tag{C.18}$$

The result can be represented as:

$$< -k|V_{1j}\widetilde{G}V_{1j}|k >= -C_j^2 [\frac{e^{2(j+1)ikz_1} + e^{2jikz_1}}{4} z_1 + \frac{i}{4k}(e^{2(j+1)ikz_1} - e^{2jikz_1}). \tag{C.19}$$

The first part of V_2^1 is given by

$$V_2^{11}(z) = \sum_{j=0}^{\infty} [\frac{C_j^2 z_1}{4} [\delta[(j+1)z_1 - z] + \delta(jz_1 - z)] - \frac{C_j^2}{2} \eta(z - jz_1)\eta[(j+1)z_1 - z]].$$

(C.20)

For $< -k|V_{1j}\widetilde{G}V_{1m}|k >\ (j > m)$, we have

$$\begin{aligned}
< -k|V_{1j}\widetilde{G}V_{1m}|k > &= \int_{-\infty}^{\infty} dz' \int_{-\infty}^{\infty} dz'' e^{ik(z'+z'')} V_{1j}\widetilde{G}_{0k}V_{1m} \\
&= C_j C_m \int_{jz_1}^{(j+1)z_1} dz' \int_{mz_1}^{(m+i)z_1} dz'' e^{ik(z'+z'')} \sin[k(z'-z'')] \\
&= C_j C_m \int_{jz_1}^{(j+1)z_1} dz' \int_{mz_1}^{(m+i)z_1} dz'' e^{ik(z'+z'')} \frac{e^{ik(z'-z'')} - e^{-ik(z'-z'')}}{2i} \\
&= -\frac{ikC_jC_m}{2} \int_{jz_1}^{(j+1)z_1} dz' \int_{mz_1}^{(m+i)z_1} dz'' (e^{2ikz'} - e^{2ikz''}) \\
&= -\frac{C_jC_mz_1}{4}[e^{2ik(j+1)z_1} - e^{2ikjz_1} - e^{2ik(m+1)z_1} + e^{2ikmz_1}].
\end{aligned} \tag{C.21}$$

The second part of V_2^1 is given by

$$\begin{aligned}
V_2^{12}(z) &= \frac{z_1}{4} \sum_{j=0}^{\infty} \sum_{m=0}^{j-1} C_jC_m[\delta[(j+1)z_1 - z] - \delta(jz_1 - z) \\
&\quad -\delta[(m+1)z_1 - z] + \delta(mz_1 - z)].
\end{aligned} \tag{C.22}$$

Then the first term of the second order is

$$\begin{aligned}
V_2^1(z) &= \sum_{j=0}^{\infty}[\frac{C_j^2 z_1}{4}[\delta[(j+1)z_1 - z] + \delta(jz_1 - z)] - \frac{C_j^2}{2}\eta(z - jz_1)\eta[(j+1)z_1 - z]] \\
&+ \frac{z_1}{4} \sum_{j=0}^{\infty} \sum_{m=0}^{j-1} C_jC_m[\delta[(j+1)z_1 - z] - \delta(jz_1 - z) \\
&\quad -\delta[(m+1)z_1 - z] + \delta(mz_1 - z)].
\end{aligned} \tag{C.23}$$

C.3.2 The second part of V_2, denoted by V_2^2

The second term of the second order:

$$\begin{aligned}
< -k|V_1R_k| - k > &= R_k \int_{-\infty}^{\infty} dz' V_1(z') \\
&= R_k[\int_0^{z_1} dz' C_0 + \int_{z_1}^{2z_1} dz' C_1 + ... + \int_{jz_1}^{(j+1)z_1} dz' C_j] \\
&= CR_k,
\end{aligned} \tag{C.24}$$

where $C = [\int_0^{z_1} dz' C_0 + \int_{z_1}^{2z_1} dz' C_1 + ... + \int_{jz_1}^{(j+1)z_1} dz' C_j]$.

The computation of the coefficient C follows:

$$\begin{aligned}
C &= [\int_0^{z_1} dz' C_0 + \int_{z_1}^{2z_1} dz' C_1 + ... + \int_{jz_1}^{(j+1)z_1} dz' C_j] \\
&= z_1[C_0 + C_1 + ... + C_j + ...] \\
&= 4z_1[(\frac{1-\sqrt{1-V_0}}{\sqrt{1-V_0}+1}) + (\frac{1-\sqrt{1-V_0}}{\sqrt{1-V_0}+1})^3 + ... + (\frac{1-\sqrt{1-V_0}}{\sqrt{1-V_0}+1})^{2j+1} + ...] \\
&= 4z_1(\frac{1-\sqrt{1-V_0}}{\sqrt{1-V_0}+1})[1 + (\frac{1-\sqrt{1-V_0}}{\sqrt{1-V_0}+1})^2 + ... + (\frac{1-\sqrt{1-V_0}}{\sqrt{1-V_0}+1})^{2j} + ...] \\
&= 4z_1(\frac{1-\sqrt{1-V_0}}{\sqrt{1-V_0}+1})\frac{1}{1-(\frac{1-\sqrt{1-V_0}}{\sqrt{1-V_0}+1})^2} \\
&= aV_0. \qquad \text{(C.25)}
\end{aligned}$$

Then, we have

$$
\begin{aligned}
V_2^2 &= -\frac{1}{\pi}\int_{-\infty}^{\infty} dk e^{-2ikz} CR_k \\
&= -\frac{aV_0}{\pi}\int_{-\infty}^{\infty} dk \frac{\sin(ak\sqrt{1-V_0})e^{-2ikz}}{\sin(ak\sqrt{1-V_0}+i\tanh^{-1}\frac{2\sqrt{1-V_0}}{2-V_0})} \\
&= \frac{2iaV_0}{\pi}\frac{1-\sqrt{1-V_0}}{\sqrt{1-V_0}+1}\int_{-\infty}^{\infty} dk \frac{\sin(ak\sqrt{1-V_0})e^{-2ikz}}{e^{-iak\sqrt{1-V_0}}[1-e^{2iak\sqrt{1-V_0}}(\frac{\sqrt{1-V_0}-1}{\sqrt{1-V_0}+1})^2]} \\
&= \frac{2iaV_0}{\pi}\frac{1-\sqrt{1-V_0}}{\sqrt{1-V_0}+1}\int_{-\infty}^{\infty} dk \frac{\sin(ak\sqrt{1-V_0})e^{-2ikz+iak\sqrt{1-V_0}}}{[1-e^{2iak\sqrt{1-V_0}}(\frac{\sqrt{1-V_0}-1}{\sqrt{1-V_0}+1})^2]} \\
&= \frac{2iaV_0}{\pi}\frac{1-\sqrt{1-V_0}}{\sqrt{1-V_0}+1}\int_{-\infty}^{\infty} dk[\sin(ak\sqrt{1-V_0})e^{-2ikz+iak\sqrt{1-V_0}}] \\
&\quad \times\sum_{j=0}^{\infty}(\frac{\sqrt{1-V_0}-1}{\sqrt{1-V_0}+1})^{2j}e^{2jiak\sqrt{1-V_0}} \\
&= \sum_{j=0}^{\infty}\frac{2iaV_0}{\pi}(\frac{1-\sqrt{1-V_0}}{\sqrt{1-V_0}+1})^{2j+1}\int_{-\infty}^{\infty} dk[\sin(ak\sqrt{1-V_0})e^{-2ikz+(2j+1)iak\sqrt{1-V_0}}] \\
&= -\sum_{j=0}^{\infty}\frac{2aV_0}{\pi}(\frac{1-\sqrt{1-V_0}}{\sqrt{1-V_0}+1})^{2j+1}\int_{-\infty}^{\infty} dk \\
&\quad \times\sin(ak\sqrt{1-V_0})\sin((2j+1)iak\sqrt{1-V_0}-2ikz) \\
&= -\sum_{j=0}^{\infty}\frac{2aV_0}{\pi}(\frac{1-\sqrt{1-V_0}}{\sqrt{1-V_0}+1})^{2j+1}\int_{-\infty}^{\infty} dk \\
&\quad \times\frac{\cos(2kz-2jak\sqrt{1-V_0})-\cos(2(j+1)ak\sqrt{1-V_0}-2kz)}{2} \\
&= -\sum_{j=0}^{\infty}\frac{aV_0}{\pi}(\frac{1-\sqrt{1-V_0}}{\sqrt{1-V_0}+1})^{2j+1}\int_{-\infty}^{\infty} dk[e^{2ik(z-ja\sqrt{1-V_0})}-e^{2ik[(j+1)ak\sqrt{1-V_0}-z]}] \\
&= -\sum_{j=0}^{\infty}aV_0(\frac{1-\sqrt{1-V_0}}{\sqrt{1-V_0}+1})^{2j+1}[\delta(z-ja\sqrt{1-V_0})-\delta[(j+1)a\sqrt{1-V_0}-z]],
\end{aligned}
\tag{C.26}
$$

C.3.3 The second order V_2

$$
\begin{aligned}
V_2(z) &= V_2^1 + V_2^2 \\
&= -\sum_{j=0}^{\infty} 8\left(\frac{1-\sqrt{1-V_0}}{\sqrt{1-V_0}+1}\right)^{4j+2}\eta(z-jz_1)\eta[(j+1)z_1-z] \\
&+ \sum_{j=0}^{\infty} 4z_1\left(\frac{1-\sqrt{1-V_0}}{\sqrt{1-V_0}+1}\right)^{4j+2}[\delta[(j+1)z_1-z]+\delta(jz_1-z)] \\
&+ \sum_{j=0}^{\infty}\sum_{m=0}^{j-1} 4z_1\left(\frac{1-\sqrt{1-V_0}}{\sqrt{1-V_0}+1}\right)^{2(j+m+1)}[\delta[(j+1)z_1-z] \\
&\quad -\delta[jz_1-z]-\delta[(m+1)z_1-z]+\delta(mz_1-z)] \\
&- \sum_{j=0}^{\infty} aV_0\left(\frac{1-\sqrt{1-V_0}}{\sqrt{1-V_0}+1}\right)^{2j+1}[\delta(z-jz_1)-\delta[(j+1)z_1-z]] \\
&= -\sum_{j=0}^{\infty} 8\left(\frac{1-\sqrt{1-V_0}}{\sqrt{1-V_0}+1}\right)^{4j+2}\eta(z-jz_1)\eta[(j+1)z_1-z] \\
&+ \sum_{j=0}^{\infty}\sum_{m=0}^{j-1} 8z_1\left(\frac{1-\sqrt{1-V_0}}{\sqrt{1-V_0}+1}\right)^{2(j+m+1)}[\delta[(j+1)z_1-z]-\delta(z-jz_1)] \\
&+ \sum_{j=0}^{\infty} 8z_1\left(\frac{1-\sqrt{1-V_0}}{\sqrt{1-V_0}+1}\right)^{4j+2)}\delta[(j+1)z_1-z]. \qquad \text{(C.27)}
\end{aligned}
$$

C.4 THE THIRD ORDER

From last two sections, we have

$$
V_1 = 4\sum_{j=0}^{\infty}\left(\frac{1-\sqrt{1-V_0}}{\sqrt{1-V_0}+1}\right)^{2j+1}\eta(z-jz_1)\eta[(j+1)z_1-z], \qquad \text{(C.28)}
$$

$$
\begin{aligned}
V_2(z) &= -\sum_{j=0}^{\infty} 8\left(\frac{1-\sqrt{1-V_0}}{\sqrt{1-V_0}+1}\right)^{4j+2}\eta(z-jz_1)\eta[(j+1)z_1-z] \\
&+ \sum_{j=0}^{\infty} 4z_1\left(\frac{1-\sqrt{1-V_0}}{\sqrt{1-V_0}+1}\right)^{4j+2}[\delta[(j+1)z_1-z]+\delta(jz_1-z)] \\
&+ \sum_{j=0}^{\infty} z_1\left(\frac{1-\sqrt{1-V_0}}{\sqrt{1-V_0}+1}\right)^{2j+1}\sum_{k=0}^{j-1}\left(\frac{1-\sqrt{1-V_0}}{\sqrt{1-V_0}+1}\right)^{2k+1} \\
&\quad \times[\delta[(k+2)z_1-z]-2\delta[(k+1)z_1-z]+\delta(kz_1-z)]] \\
&- \sum_{j=0}^{\infty} aV_0\left(\frac{1-\sqrt{1-V_0}}{\sqrt{1-V_0}+1}\right)^{2j+1}[\delta(z-jz_1)-\delta[(j+1)z_1-z]].
\end{aligned}
\tag{C.29}
$$

The third order:

$$
\begin{aligned}
< -k|V_3|k > &= - < -k|V_2\widetilde{G}_{0k}V_1|k > - < -k|V_1\widetilde{G}_{0k}V_2|k > \\
&\quad - < -k|V_1\widetilde{G}_{0k}V_1\widetilde{G}_{0k}V_1|k > \\
&- R_k < -k|V_2|-k > -R_k < -k|V_1\widetilde{G}_{0k}V_1|-k > .
\end{aligned}
\tag{C.30}
$$

Let us only consider the heaviside terms: Let

$$
V_1 = \sum_{j=0}^{\infty} C_j\eta(z-jz_1)\eta[(j+1)z_1-z]. \tag{C.31}
$$

$$
V_2'(z) = -\sum_{j=0}^{\infty}\frac{C_j^2}{2}\eta(z-jz_1)\eta[(j+1)z_1-z]. \tag{C.32}
$$

The first term of the third order is

$$
- < -k|V_{2j}\widetilde{G}_{0k}V_{1j}|k > = -\frac{ik}{2}C_j^3[\frac{e^{2(j+1)ikz_1}+e^{2jikz_1}}{4}z_1+\frac{i}{4k}(e^{2(j+1)ikz_1}-e^{2jikz_1})]. \tag{C.33}
$$

Then

$$
V_3^1(z) = \sum_{j=0}^{\infty}\frac{C_j^3}{4}\eta(z-jz_1)\eta[(j+1)z_1-z]. \tag{C.34}
$$

Similarly, the second term is

$$V_3^2(z) = \sum_{j=0}^{\infty} \frac{C_j^3}{4} \eta(z - jz_1)\eta[(j+1)z_1 - z]. \tag{C.35}$$

For the third term:

$$\begin{aligned} - < -k|V_{1j}\widetilde{G}_{0k}V_{1j}\widetilde{G}_{0k}V_{1j}|k > &= -C_j^3[\frac{3}{16}(e^{2ikz_1} + e^{2ikz_2})(z_2 - z_1) \\ &\quad -\frac{3}{16ik}(e^{2ikz_2} - e^{2ikz_1}) \\ &\quad -\frac{ik}{16}(e^{2ikz_2} - e^{2ikz_1})(z_2 - z_1)^2]. \end{aligned} \tag{C.36}$$

Then

$$V_3^3(z) = -\sum_{j=0}^{\infty} \frac{3C_j^3}{8} \eta(z - jz_1)\eta[(j+1)z_1 - z]. \tag{C.37}$$

The fourth term only contains delta function terms, so we neglect it.

The fifth order is

$$\begin{aligned} V_3^5(2k) &= -\sum_{j=0}^{\infty} R_k < -k|V_{1j}\widetilde{G}_{0k}V_{1j}| - k > -\sum_{j=1}^{\infty}\sum_{m=0}^{j-1} R_k < -k|V_{1j}\widetilde{G}_{0k}V_{1m}| - k > \\ &= -\sum_{j=0}^{\infty} R_k[\frac{C_j^2}{4}z_1 + \frac{ik}{4}C_j^2 z_1^2 + \frac{1}{8ik}C_j^2(e^{2ikz_1} - 1)] \\ &\quad + \sum_{j=1}^{\infty}\sum_{m=0}^{j-1} R_k[\frac{ik}{2}C_jC_m z_1^2] \\ &\quad -\frac{1}{8ik}C_jC_m(2e^{2ik(j-m)z_1} - e^{2ik(j+m-1)z_1} - e^{2ik(j+1-m)z_1})], \end{aligned} \tag{C.38}$$

we only consider the heaviside terms

$$\begin{aligned} V_3^5(2k) &= -\sum_{j=0}^{\infty} R_k \frac{1}{8ik}C_j^2(e^{2ikz_1} - 1) \\ &\quad -\sum_{j=1}^{\infty}\sum_{m=0}^{j-1} R_k \frac{1}{8ik}C_jC_m(2e^{2ik(j-m)z_1} - e^{2ik(j+m-1)z_1} - e^{2ik(j+1-m)z_1}). \end{aligned} \tag{C.39}$$

Then

$$
\begin{aligned}
V_3^5(z) &= \sum_{j=0}^{\infty}\sum_{n=0}^{\infty}\frac{C_j^2 C_n}{16}[\eta(z-nz_1)\eta[(n+1)z_1-z]-\eta[z-(n+1)z_1]\eta[(n+2)z_1-z] \\
&\quad -\sum_{j=1}^{\infty}\sum_{m=0}^{j-1}\sum_{n=1}^{\infty}C_jC_mC_n[\eta[z-(n+j-m-1)z_1]\eta[(n+j-m-1)z_1-z] \\
&\quad +\eta[z-(n+j-m+1)z_1]\eta[(n+j-m+2)z_1-z] \\
&\quad -2\eta[z-(n+j-m)z_1]\eta[(n+j-m+1)z_1-z]. \qquad \text{(C.40)}
\end{aligned}
$$

Summing all the terms, we obtain the heaviside terms of the third order:

$$
\begin{aligned}
V_3'(z) &= \sum_{n=0}^{\infty}\frac{C_n^3}{8}\eta(z-nz_1)\eta[(n+1)z_1-z] \\
&+ \sum_{j=0}^{\infty}\sum_{n=0}^{\infty}\frac{C_j^2 C_n}{16}[\eta(z-nz_1)\eta[(n+1)z_1-z]-\eta[z-(n+1)z_1]\eta[(n+2)z_1-z] \\
&- \sum_{j=1}^{\infty}\sum_{m=0}^{j-1}\sum_{n=0}^{\infty}C_jC_mC_n[\eta[z-(n+j-m-1)z_1]\eta[(n+j-m-1)z_1-z] \\
&\quad +\eta[z-(n+j-m+1)z_1]\eta[(n+j-m+2)z_1-z] \\
&\quad -2\eta[z-(n+j-m)z_1]\eta[(n+j-m+1)z_1-z]. \qquad \text{(C.41)}
\end{aligned}
$$

APPENDIX D INVERSE ACOUSTIC SCATTERING SERIES USING THE VOLTERRA RENORMALIZATION OF LIPPMANN-SCHWINGER EQUATION. SEG ABSTRACT 2013.

In this appendix, we reproduce the abstract that has been accepted for the technical program at the SEG (Society of Exploration Geophysicists) 2013 annual conference in Houston.

Inverse acoustic scattering series using the Volterra renormalization of the Lippmann-Schwinger equation

Anne-Cecile Lesage[*†], *Jie Yao*[†], *Roya Eftekhar*[†], *Fazle Hussain*[‡] *and Donald J. Kouri*[†]
[†]*University of Houston, TX,* [‡]*Texas Tech University at Lubbock, TX*

SUMMARY

We report the extension of the inverse acoustic scattering approach presented in (Kouri and Vijay, 2003) from the use of both reflection and transmission data (R_k/T_k) to the sole use of the reflection data (R_k). The approach consists in combining two ideas: the renormalization of the Lippmann-Schwinger equation to obtain a Volterra equation framework (Kouri and Vijay, 2003) and the formal series expansion using reflection coefficients (Moses, 1956). The benefit of formulating acoustic scattering in terms of a Volterra kernel is substantial. Indeed the corresponding Born-Neumann series solution is absolutely convergent independent of the strength of the coupling characterizing the interaction. We derive new inverse acoustic scattering series for reflection data which we evaluate for test cases both analytically and numerically (Dirac-δ interaction and the square well or barrier). Our results compare well to results obtained by (Weglein *et al.*, 2001) for the square barrier and to previous results obtained in (Kouri and Vijay, 2003) using both transmission and reflection data.

INTRODUCTION

Inverse acoustic scattering methods pioneered by Weglein and co-workers (Weglein *et al.*, 1997, 2001) have a significant advantage in comparison to other data inversion methods like Full Waveform Inversion (Tarantola, 1984; Pratt, 1999). Indeed they are the only methods for which the actual and the estimated reference are not assumed to be equal. The inversion for medium properties uses only reflection data and reference medium properties. The methods are non-iterative in the sense that the reference medium is never updated. The approach uses the Born-Neumann power series solution of the acoustic Lippmann-Schwinger equation and a related expansion of the interaction in "orders of data" (Jost and Kohn, 1952; Moses, 1956; Razavy, 1975).

Nevertheless the approach is limited by the finite radius of convergence of the Born-Neumann series of the acoustic Lippmann Schwinger equation. Moreover, it depends on the square of the frequency. Despite this limitation, Weglein and co-workers have made significant progress by separating the Born-Neumann series terms into "task-related" subseries. In (Weglein *et al.*, 1997), they derived an inverse scattering method to separate series for internal multiple events from the one for primaries (reflector imaging subseries). In (Weglein *et al.*, 2001), they illustrated the method for 1D acoustic scattering for a square well assuming multiples have been removed.

In (Kouri and Vijay, 2003), Kouri and co-workers proposed to apply the renormalization transformation of the Lippmann-Schwinger equation into a Volterra equation form to tackle the convergence limitation of the inverse acoustic scattering series. The Volterra form allows for the derivation of a Born-Neumann expansion that converges absolutely independent of the strength of the scattering interaction. It results from the property that the "Fredholm determinant" of the corresponding integral equation can be shown to be equal to one. Nevertheless, the inverse series was derived for the case of R_k/T_k data which is not useful for oil prospecting. This paper provides the extension of the approach to the case where one only has reflection data. We compare the results of this extension to those of R_k/T_k data (Kouri and Vijay, 2003) and those of Weglein and co-workers (Weglein *et al.*, 2001).

INVERSE ACOUSTIC SCATTERING THEORY

Renormalization of the Lippmann-Schwinger equation

Here we illustrate our method for a 1-D acoustic medium but the approach is completely general and extends to three dimensions. For a normal incident wave upon a 1-D acoustic medium, the pressure $P(z,\omega)$ is governed in the frequency-domain formulation by the Helmholtz equation:

$$(\frac{\partial}{\partial z^2}+\frac{\omega^2}{c_0^2(z)})P = \frac{\omega^2}{c_0^2}(1-\frac{c_0^2(z)}{c^2(z)})P \quad (1)$$

$$(\frac{\partial}{\partial z^2}+k^2)P = k^2VP \quad (2)$$

with $c_0(z)$ the reference acoustic P-wave velocity, c the velocity to invert for, $k^2=\frac{\omega^2}{c_0^2}$ and $V=(1-\frac{c_0^2}{c^2})$ the spatial part of the perturbation interaction.

The Lippmann-Schwinger integral equation for the pressure reads as follows:

$$P_k^+(z)=e^{ikz}-\frac{i}{2k}\int_{-\infty}^{\infty}dz'e^{ik|z-z'|}k^2V(z')P_k^+(z) \quad (3)$$

with the usual causal free Green function (including the k^2 factor coming from the interaction), given as:

$$G_{0k}^+=-\frac{ik}{2}e^{ik|z-z'|}. \quad (4)$$

The renormalization transformation of the Lippmann-Schwinger equation to a Volterra equation results from eliminating the $|z-z'|$ argument in the free Green's function in equation (3). This is done by dividing the integration over z' into segments from $-\infty$ to z and from z to ∞:

$$P_k^+(z) = e^{ikz}-\frac{ik}{2}\int_{-\infty}^{z}dz'e^{ik(z-z')}V(z')P_k^+(z')$$

$$-\frac{ik}{2}\int_z^\infty dz' e^{-ik(z-z')}V(z')P_k^+(z') \qquad (5)$$

One then adds and substracts $-\frac{ik}{2}\int_{-\infty}^z dz' e^{ik(z'-z)}V(z')P_k^+(z')$ to obtain a Volterra equation.

$$\begin{aligned} P_k^+(z) &= e^{ikz} - \frac{ik}{2}\int_{-\infty}^\infty dz' e^{ik(z'-z)}V(z')P_k^+(z) \\ &\quad -\frac{ik}{2}\int_{-\infty}^z dz'[e^{ik(z-z')} - e^{-ik(z-z')}]V(z')P_k^+(z') \\ P_k^+(z) &= e^{ikz} + R_k e^{-ikz} + k\int_{-\infty}^z dz' sink(z-z')V(z')P_k^+(z') \end{aligned} \qquad (6)$$

The new Green operator $\tilde{G}_{0k}$ is given by:

$$\tilde{G}_{0k}(z,z'') = ksin[k(z-z'')] \times \eta(z-z'') \qquad (7)$$

with $\eta(z)$ being the heaviside function.
Because of the triangular nature of $\tilde{G}_{0k}$, the Born-Neumann series converges absolutely and uniformly on any compact set of z, provided V decays faster than $\frac{1}{z^2}$ for large z, and has only integrable singularities.

Inverse series for R_k/T_k data

We recall the Volterra inverse series in orders of $\tilde{T}$ the auxiliary transition operator (cf. (Kouri and Vijay, 2003)):

$$\tilde{T} = \sum_{n=0}^\infty (V\tilde{G}_{0k})^n V \qquad (8)$$

We express V as a power series in orders of $\tilde{T}$ (cf Weglein) $V = \sum_{j=1}^\infty \tilde{\varepsilon}^j \tilde{V}_j$. Then we collect coefficients of each power of $\tilde{\varepsilon}^j$

$$\tilde{\varepsilon}^1 \quad : \quad \tilde{T} = \tilde{V}_1, \qquad (9)$$

$$\tilde{\varepsilon}^2 \quad : \quad 0 = \tilde{V}_2 + \tilde{V}_1\tilde{G}_{0k}\tilde{V}_1, \qquad (10)$$

$$\tilde{\varepsilon}^3 \quad : \quad 0 = \tilde{V}_3 + \tilde{V}_2\tilde{G}_{0k}\tilde{V}_1 + \tilde{V}_1\tilde{G}_{0k}\tilde{V}_2 + \tilde{V}_1\tilde{G}_{0k}\tilde{V}_1\tilde{G}_{0k}\tilde{V}_1, \qquad (11)$$

etc., with $\tilde{V}_1(-k,k) = \frac{iR_k}{k\pi T_k}$.

Inverse series for R_k data

To develop an approach to inversion using solely the reflection data R_k, we consider the following expression (Moses, 1956):

$$R_k = \frac{-ik}{2}\int_{-\infty}^\infty dz' e^{ikz'}V(z')P_k^+(z') \qquad (12)$$

with

$$P_k^+(z) = e^{ikz} + R_k e^{-ikz} + k\int_{-\infty}^z dz' sin[k(z-z')]V(z')P_k^+(z') \qquad (13)$$

We search for a solution of the form:

$$P_k^+(z) = U_{1k}(z) + R_k U_{2k}(z) \qquad (14)$$

which gives

$$\begin{aligned} U_{1k}(z) &= e^{ikz} + k\int_{-\infty}^z dz' sin[k(z-z')]V(z')U_{1k}(z') \\ U_{2k}(z) &\equiv U_{1k}^*(z') \end{aligned} \qquad (15)$$

We now can write

$$R_k = \frac{-ik}{2}\int_{-\infty}^\infty dz' e^{ikz'}V(z')[U_{1k}(z') + R_k U_{1k}^*(z')] \qquad (16)$$

We write the Born-Neumann series

$$U_{1k}(z) = \sum_{n=0}^\infty (\tilde{G}_{0k}V)^n|k> \qquad (17)$$

We substitue in equation (16):

$$\begin{aligned} R_k &= \frac{-ik}{2}\int_{-\infty}^\infty dz' e^{ikz'}V(z')[\sum_{n=0}^\infty (\tilde{G}_{0k}V)^n|k> \\ &+ R_k\sum_{n=0}^\infty (\tilde{G}_{0k}V)^n|-k>] \end{aligned} \qquad (18)$$

Next, assuming that R_k is the sole measured data, we express the perturbation as $V(z) = \sum_{j=1}^\infty V_j(z)$ where V_1 is first order in R_k, ..., V_j is jth order in R_k.

$$\begin{aligned} R_k = \frac{-ik}{2}\int_{-\infty}^\infty dz' e^{ikz'}\sum_{n=1}^\infty V_j(z)[\sum_{n=0}^\infty (\tilde{G}_{0k}\sum_{n=1}^\infty V_j(z))^n|k> \\ +R_k\sum_{n=0}^\infty (\tilde{G}_{0k}\sum_{n=1}^\infty V_j(z))^n|-k>] \end{aligned} \qquad (19)$$

with $|k>\sim e^{ikz}$, $|-k>\sim e^{-ikz}$. This leads to the following expressions which determine V_1, V_2, ...
The first order is given as:

$$\begin{aligned} R_k &= \frac{-ik}{2}\int_{-\infty}^\infty dz' < -k|V_1(z')|k> \\ V_1(z) &= 2\int_{-\infty}^\infty dk W_1(k)e^{-2ikz} \\ W_1(k) &= \frac{R(k)}{-\pi ik} \end{aligned} \qquad (20)$$

The second order is given as:

$$\begin{aligned} V_2(z) &= -2\int_{-\infty}^\infty dk W_2(k)e^{-2ikz} \\ W_2(k) &= \frac{1}{2\pi}\Big[\int_{-\infty}^\infty dz' < -k|V_1(z')\tilde{G}_{0k}V_1|k> \\ &+ \int_{-\infty}^\infty dz' V_1(z')R_k\Big] \end{aligned} \qquad (21)$$

The third order is given as:

$$\begin{aligned} V_3(z) &= -2\int_{-\infty}^\infty dk W_3(k)e^{-2ikz} \\ W_3(k) &= \frac{1}{2\pi}\Big[\int_{-\infty}^\infty dz' < -k|V_2(z')\tilde{G}_{0k}V_1|k> \\ &+ \int_{-\infty}^\infty dz' < -k|V_1(z')\tilde{G}_{0k}V_2|k> + \int_{-\infty}^\infty dz' < -k|V_1(z')(\tilde{G}_{0k}V_1)^2|k> \\ &+ \int_{-\infty}^\infty dz' < -k|V_2(z')R_k|-k> + \int_{-\infty}^\infty dz' < -k|V_1(z')R_k\tilde{G}_{0k}V_1|-k>\Big] \end{aligned} \qquad (22)$$

We point out that the V_1 expression, equation (20), is the same as arises in (Weglein *et al.* 2001). The higher order terms differ in two ways. First they contain the triangular Green function $\tilde{G}_{0k}$. Secondly, there are extra terms that also contain the data R_k.

ANALYSIS OF NUMERICAL AND ANALYTICAL RESULTS FOR THE INVERSE SERIES

We test the new Volterra inverse acoustic scattering series in R_k (equations (19, 20, 21, 22)) on two cases: the Dirac δ-function interaction and the case of sound scattering by either a square well or barrier.

Application to the Dirac δ-function interaction

In the case of the application to scattering by the Dirac δ-function interaction located at depth $z = z_0$, the reflection and transmission coefficients can be computed analytically. They are given as follows:

$$\begin{aligned} R_k &= \frac{-ik\gamma}{2+ik\gamma}e^{2ikz_0} \\ T_k &= \frac{2}{2+ik\gamma}. \end{aligned} \tag{23}$$

Using the Volterra inverse series in R_k and T_k (equations (8, 9,10,11)), we recall the results obtained in (Kouri and Vijay, 2003):

$$\tilde{V}_1(z) = \gamma\delta(z-z_0),\ \tilde{V}_2(z) = 0. \tag{24}$$

Thus, this Volterra series converges to the exact answer in a single term, with all higher terms being zero.

Using the Volterra inverse series in R_k, we can demonstrate for the first three orders computing analytically the integrals of equations (20, 21, 22), that:

$$V_1(z) = 4e^{-\frac{4}{\gamma}(z_0-z)}\eta(z_0-z) \tag{25}$$

$$V_2(z) = 2\gamma\delta(z_0-z) - 16e^{-\frac{8}{\gamma}(z_0-z)}\eta(z_0-z) \tag{26}$$

$$\begin{aligned} V_3(z) &= \frac{11}{2}\gamma\delta(z_0-z) + 63e^{-\frac{12}{\gamma}(z_0-z)}\eta(z_0-z) \\ &\quad -e^{\frac{4}{\gamma}(z-z_0)}\eta(z-z_0) + \frac{3\gamma^2}{8}\delta'(z-z_0) \end{aligned} \tag{27}$$

The new Volterra inverse series has not yet fully converged after three terms. The analytical and numerical evaluation of higher order terms will be the goal of further investigations. However, we anticipate that one will obtain higher derivatives of the Dirac-δ function which, as is the case in the approach of (Weglein *et al.* 2001) for the square barrier, are associated with a Taylor expansion of Heaviside functions.

Application to the square well or barrier

In the case of the application to scattering by a finite width square well or barrier ($V(z) = V_0\eta(z)\eta(a-z)$), the reflection and transmission coefficients can again be computed analytically. They are given as follows:

$$R_k = \frac{V_0}{(2-V_0)+2i\sqrt{1-V_0}\cot(ak\sqrt{1-V_0})} \tag{28}$$

$$T_k = \frac{2\sqrt{1-V_0}ie^{-ika}}{V_0 sin(ka\sqrt{1-V_0})}R_k \tag{29}$$

V_0 is the perturbation interaction amplitude and a is its width. The case $V_0 < 0$ corresponds to a square well (decrease of the acoustic velocity so that $c < c_0$). The case $0 < V_0 < 1$ corresponds to a barrier.

Using the Volterra inverse series in R_k and T_k (equations (8, 9,10,11)), we recall the results obtained in (Kouri and Vijay, 2003):

$$\tilde{V}_1(z) = \frac{V_0}{\sqrt{1-V_0}}\eta(z-z_{min})\eta(z_{max}-z) \tag{30}$$

with $z_{min} = \frac{a}{2}(1-\sqrt{1-V_0})$ and $z_{max} = \frac{a}{2}(1+\sqrt{1-V_0})$.

Using the new Volterra inverse series in R_k, we can compute the first order V_1:

$$V_1(z) = 2\int_{-\infty}^{\infty} dk W^1(k)e^{-2ikz} \tag{31}$$

$$\begin{aligned} W^1(k) &= \frac{R_k}{-\pi ik} \\ &= \frac{iV_0\sin(ak\sqrt{1-V_0})}{\pi k[(2-V_0)\sin(ak\sqrt{1-V_0})+2i\sqrt{1-V_0}\cos(ak\sqrt{1-V_0})]} \end{aligned} \tag{32}$$

We can evaluate it numerically by a trapezoidal rule quadrature from the following equation:

$$V_1(z) = \frac{2V_0}{\pi(V_0-2)^2}\int_{-\infty}^{\infty} dk \sin(ak\sqrt{1-V_0}) \times \frac{2\sqrt{1-V_0}\cos(ak\sqrt{1-V_0})\cos(2kz)+(2-V_0)\sin(ak\sqrt{1-V_0})\sin(2kz)}{k[1-\frac{V_0^2}{(V_0-2)^2}\cos^2(ak\sqrt{1-V_0})]} \tag{33}$$

We observe that V_1 can be derived analytically as a infinite series of decreasing height barriers:

$$V_1(z) = \sum_{n=1}^{\infty} C_n\eta(z)\eta(z_n) \tag{34}$$

with $z_n = na\sqrt{1-V_0}$. The C_n expression can be obtained from equation (33) by expanding the denominator with the Taylor series $\frac{1}{1-x} = \sum_0^\infty x^n$. In practice, we use $m = 4$ as truncation order which gives a good convergence. For different values of V_0 (cf Figures 1, 2), we compare the plots of the exact barrier, the first order term $\tilde{V}_1(z)$ obtained through the Volterra inverse series with R_k, T_k data and the first order term $V_1(z)$ obtained through the new Volterra inverse series in R_k both numerically and analytically (equations (33, 34)).

As for the Volterra inverse series for R_k/T_k (Kouri and Vijay, 2003), the first-order result has the correct analytical form of a square well or barrier but it has incorrect width and height (or depth). For a barrier ($0 < V_0 < 1$), the first order result using only R_k has higher barrier than the true one (cf Figures 1). While for a well ($V_0 < 0$), the first order result has higher barrier than the true one (cf Figure 2). The height is slightly closer to the exact value than for the R_k/T_k data results. The R_k/T_k series spreads the error in the width equally onto both sides of

the barrier while the R_k series has all the error on the right (this is the same result as Weglein and co-workers (Weglein *et al.*, 2001)).

Using equation (21), we evaluate the second order $V_2(z)$ for the R_k Volterra inverse series. We compute the first term $V_{21}(z)$ and the second term $V_{22}(z)$ analytically with:

$$\begin{aligned}
V_{21}(z) &= -2\int_{-\infty}^{\infty} dk W_{12}(k) e^{-2ikz} \\
W_{12}(k) &= \frac{1}{2\pi}\int_{-\infty}^{\infty} dz' \int_{-\infty}^{\infty} dz" e^{ik(z'+z")} V_1(z') \widetilde{G}_{0k}(z',z") V_1(z") \\
V_{21}(z) &\approx \sum_{j=0}^{3} (-\frac{C_j^2}{2}\eta(z-z_j)\eta(z_{j+1}-z) \\
&+ \frac{C_j^2 z_1}{4}[\delta(z_{j+1}-z)+\delta(z_j-z)] \\
&+ \frac{C_j z_1}{4}\sum_{k=0}^{j-1} C_k[\delta(z_{k+2}-z)-2\delta(z_{k+1}-z)+\delta(z_k-z)])
\end{aligned} \tag{35}$$

$$\begin{aligned}
V_{22}(z) &= -2\int_{-\infty}^{\infty} dk W_{22}(k) e^{-2ikz} \\
W_{22}(k) &= \frac{1}{2\pi}\int_{-\infty}^{\infty} dz' V_1(z') R_k. \\
V_{22}(z) &= -\sum_{j=0}^{3} D(\frac{1-\sqrt{1-V_0}}{\sqrt{1-V_0}+1})^{2j+1}[\delta(z-z_j)-\delta(z_{j+1}-z)]
\end{aligned} \tag{36}$$

with $D = z_1 \sum_{j=0}^{3} C_j$.

Figure 3 shows the plot of $V_{21}(z)$ (Heaviside part). We observe that the heaviside part of $V_{21}(z)$ partially corrects the error on the height barrier. $V_{21}(z)$ and $V_{22}(z)$ both contain Dirac-δ functions which correspond to Taylor expansion of Heaviside functions. As mentionned in (Weglein *et al* 2001), those terms will correct for the barrier/well width error.

CONCLUSION

We have reported the extension of the inverse acoustic scattering approach presented in (Kouri and Vijay, 2003) to the sole use of the reflection data R_k. The first two terms are encouraging but higher order terms are needed to clearly demonstrate convergence. Future works will include the computation both analytically and/or numerically of higher order terms and extending the Volterra approach to 2D and 3D.

ACKNOWLEDGMENTS

We thank Total and PGS for their support and the authorization to present this work. The author D.J.K. thanks A.B. Weglein for introducing him to inverse scattering based on the Born-Neumann expansion.

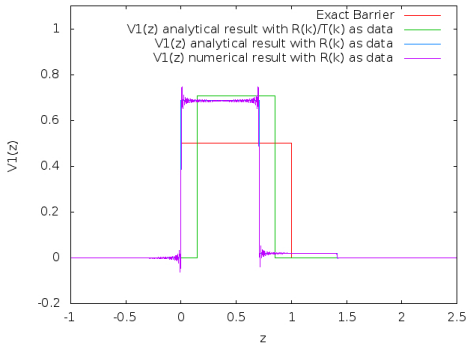

Figure 1: *Comparison of $V_1(z)$ obtained through the new Volterra inverse series in R_k, $\tilde{V}_1(z)$ obtained through the Volterra inverse series with R_k and the exact barrier. Square barrier test case: $V_0 = 0.5$, $a = 1.0$.*

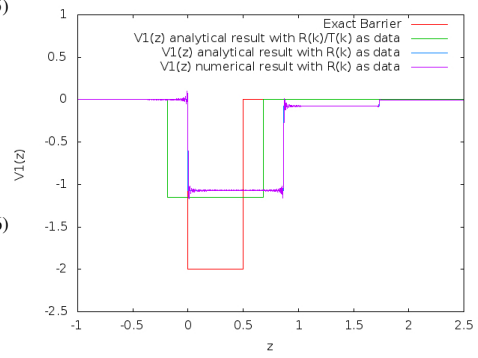

Figure 2: *Square barrier test case: $V_0 = -2.0$, $a = 0.5$.*

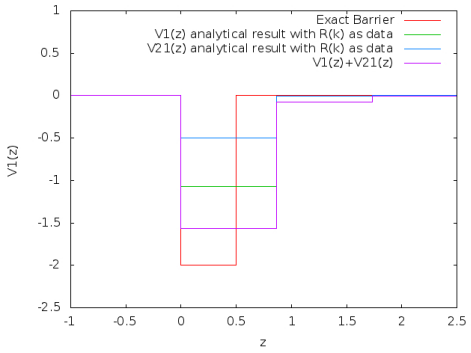

Figure 3: *Comparison of $V_1(z) + V_2(z)$ obtained through the new Volterra inverse series in R_k and the exact barrier. Square barrier test case: $V_0 = -2.0$, $a = 0.5$.*